

University Degree in Energy Engineering
2017-2018

Bachelor Thesis

“Experimental design to study the
performance of a solar cell at high
altitude”

Irene Pedrazuela Blanco

Tutor

Carolina Marugán Cruz



This work is licensed under Creative Commons **Attribution – Non Commercial – Non Derivatives**

ABSTRACT

This bachelor thesis is focused on the previous theoretical and experimental study of an array of four monocrystalline solar cells that are going to be implemented on a high altitude balloon. The balloon will carry the cells through the troposphere and part of the stratosphere. It covers the theoretical background of solar energy, with a detailed explanation on how electricity is generated using photovoltaic cells and the factors that modify the radiation while passing through the layers of the Earth atmosphere.

An experimental design has been performed in order to be able to measure voltage and current of solar cells on the balloon and to characterize the cells, by obtaining the curves of current versus voltage, the power and the changes in open circuit voltage and short circuit current with temperature and radiation. The characteristic I-V and power curves have been compared to the ideal ones, obtained with the implementation of the correlations between voltage and current in a Matlab script.

Furthermore, a theoretical approach of the insulation of the cells has been made, as the temperature gradient decreases with altitude and affects the performance of the solar cells. Also, the changes in radiation have been studied in order to decide whether the implementation of filters are necessary for protecting the cells from excessive levels of radiations.

All the experiments have been carried out by developing a code with Arduino and Matlab softwares.

Keywords: *Solar cells, high altitude balloon, experimental design, radiation, voltage, current, power, efficiency, insulation, filters, Arduino, Matlab.*

ACKNOWLEDGMENTS

I would like to specially thank my tutor, Carolina Marugán, for allowing me to participate in this project and helping me through it and my friend Carolina Nicolás for letting me borrow her Arduino kit for doing the experiments and for introducing me to the software.

Also, I want to thank my family, friends and basketball teammates for all the support they have given me through these months along with my classmates of Energy Engineering that have been by my side during my studies at the University Carlos III.

CONTENTS

1. INTRODUCTION.	1
1.1. Objective	1
1.2. The high altitude balloon project	1
2. SOLAR RADIATION.	4
2.1. The Sun	4
2.2. Radiation	5
2.3. The Earth-Sun relations	8
2.3.1. Radius Earth-Sun estimation	8
2.3.2. Variations in Extraterrestrial radiation	9
2.3.3. Solar Angles	10
2.3.4. Solar Time	12
2.3.5. Clearness Index.	13
2.3.6. Albedo	13
3. THE EARTH ATMOSPHERE	14
3.1. Chemical composition of the atmosphere	14
3.2. Layers of the atmosphere	15
4. PHOTOVOLTAIC CELLS	18
4.1. The photoelectric effect	18
4.2. Composition of PV cells.	19
4.3. Characteristic parameters of a PV cell	21
4.4. Types of PV cells.	23
5. DEVICE SELECTION AND IMPLEMENTATION.	26
5.1. Solar Cells Selection.	26
5.2. Assembly and performance	28
5.3. Implementing Arduino.	30
5.3.1. Voltage measurement	31
5.3.2. Current measurement	32
5.3.3. Load variations	33

5.3.4. Final circuit	34
5.3.5. Arduino in the high altitude balloon	34
6. THEORETICAL MODEL	36
6.1. Matlab simulation to predict the I-V curve.	36
6.2. Power curve.	37
6.3. I-V curve shifts	37
7. EXPERIMENTAL SETUP	38
7.1. Characteristic I-V curve	38
7.2. Incidence angle variation	39
7.3. Temperature variation	39
8. RESULTS	40
8.1. Characteristic I-V curve	40
8.2. Incidence angle variation	41
8.3. Temperature variation	42
8.4. Load variation	43
9. THERMAL INSULATION OF THE DEVICE.	44
9.1. Parameters that affect the temperature of a solar cell	44
9.2. Insulation model	45
9.3. Manufacturers selection	47
10. RADIATION FILTERS	49
11. COSTS ANALYSIS	52
12. CONCLUSIONS.	54
13. FUTURE WORKS.	56
BIBLIOGRAPHY.	58
A. ANNEX I	62

LIST OF FIGURES

2.1	Layers of the Sun	5
2.2	Electromagnetic Spectrum [7]	6
2.3	Solar spectral irradiance [9]	6
2.4	Solar Radiation through the atmosphere [10]	7
2.5	Solstices and Equinoxes [11]	8
2.6	Variation of G_{on} through the year [3]	9
2.7	Solar Angles	10
2.8	Equation of time throughout the year [3]	12
3.1	Atmosphere layers and temperature gradient [17]	16
4.1	Apparatus photoelectric effect [20]	18
4.2	N-type and P-type semiconductor materials [23]	20
4.3	Equivalent circuit of a solar cell	21
4.4	I-V curve of a solar cell [27]	23
4.5	Monocrystalline, Polycrystalline and Amorphous solar cells [29]	24
5.1	I-V curve of one Mr. Watt solar cell	28
5.2	Schematic of the array of solar cells	28
5.3	Upper and lower sides of a solar cell with tabbing wire	29
5.4	Bus and tabbing wire welding	29
5.5	Voltage performance test	30
5.6	Scheme of the structure in Matlab	31
5.7	Voltage connections in Arduino UNO	32
5.8	Current sensor connections in Arduino UNO	32
5.9	Potentiometer schemes	33
5.10	Final circuit connections scheme	34
5.11	Types of Arduino UNO feeding solutions	34
5.12	Arduino UNO to microSD reader connections [36]	35

6.1	Theoretical I-V curve for an array of four solar cells	36
7.1	Final installation	38
8.1	I-V curve comparison	40
8.2	Power curve comparison	41
8.3	V_{oc} and I_{sc} changes with slope angle	42
8.4	V_{oc} and I_{sc} changes with cell temperature	42
8.5	V_{oc} and I_{sc} changes with load variations	43
9.1	Solar cells insulation array	46
10.1	Absorbers in the atmosphere [43]	49
10.2	Mixing ratio of absorbers with altitude [15]	50
10.3	Reduction of direct radiation [44]	50
12.1	Experimental I-V and power curves	54
13.1	Payload measures	56

LIST OF TABLES

3.1	Main components of the homosphere	14
3.2	Main components of the heterosphere	15
5.1	Technical specifications of a solar cell [33]	27
9.1	Insulation materials	47
9.2	Insulators manufacturers	48
10.1	Wavelengths of Sun radiation	51
11.1	Material costs	52
11.2	Tool costs and amortization	52
11.3	Human resource costs	53
11.4	Total costs	53

1. INTRODUCTION

Since the Industrial Revolution, the society has been looking for methods to generate electricity in the most efficient and cheapest ways. The oil crisis and the overuse of fossil fuels led society to find alternative procedures for getting electricity, allowing renewable energies to become important. One of the most important natural resources that can be used to generate the energy needed is the Sun. With the discovery of the photoelectric effect, people realized that the Sun radiation could be transformed into electricity by simply joining two semiconductor materials, one lacking positive charges and the other lacking negative charges. When the solar radiation strikes in the materials, the electrons flow from one material to another creating current.

Additionally, the discovery and development of batteries in the recent years have allowed the storing of the energy surplus for using it in another moment, for example, in the case of photovoltaics, when there is a shortage of electricity because there is no Sun.

1.1. Objective

The objective of this bachelor thesis is to study and test the performance of monocrystalline photovoltaic cells so they can operate at the maximum possible efficiency at high altitude. It includes all the previous research and calculations in order to attach the solar cells to a high altitude balloon and in order to know the variation of voltage, current, efficiency and power with radiation and temperature.

Also, the study of the theoretical background of insulation types for solar cells and radiation filters

1.2. The high altitude balloon project

Researches in photovoltaics increased rapidly over the years and have been introduced in other technologies to improve the operation. A good example of this are the satellites that orbit around the Earth. Many satellites have been launched to the different layers of the atmosphere, or even to the outer space, for scientific, meteorological or communication purposes.

In 1958, the first satellite to use solar energy was sent off to space and it is still orbiting around the Earth [1]. The light weight of the solar cells along with the large amount of radiation that can be taken advantage from, make solar cells the optimum way to obtain electricity for the operation of these machines that need a reliable and durable energy source. Another use of solar cells is to supply electricity to weather or high altitude balloons that scientists launch to the higher layers of the atmosphere to study parameters

like solar radiation, temperature gradients or the concentration of certain substances.

Last September, 2017, the Carlos III University of Madrid started a project to develop a high altitude balloon in order to involve students in the creation, calculations and experiments that can be carried out in this kind of work.

The high altitude balloon is a latex balloon that will be released free until it reaches the stratosphere (around 30 kilometers vertical from the Earth surface). Initially, the project was divided in different groups of people in order to develop the different aspects of the launch:

- Aerodynamics
- Security
- Communications
- Experiments

The aerodynamics group had to study the different types of balloon materials that can be used (latex, totex, polyethylene), the type of balloon (open or closed), how to predict the trajectory and the gas needed to fill the balloon. Secondly, the security group investigated and determined the design of the parachute and how to implement it so it will open when the balloon bursts. Then, the communications group decided how we were going to collect the data of the experiments carried out in the box that will be tied up to the balloon and the tracking systems.

Two experiments are going to be performed by members of the project. Besides measuring temperature, humidity and height, we are going to cover the study of other parameters:

- Aerodynamics of the fall
- Performance of solar cells at high altitude

This bachelor thesis covers the previous calculations and tests in order to get the voltage, current, power and efficiency data at different altitudes. It includes the development of the code and circuit disposition to measure and keep the parameters in the balloon with the help of softwares Arduino and Matlab. The experiments that are carried out include obtaining the I-V curve of the selected solar cells both theoretical and practical, a theoretical approach of the needed insulation and radiation filters and the final implementation in the high altitude balloon.

The structure of the present document is divided in three main parts:

- The **first part** is an approach to the theoretical background, that has been studied and that is needed for the definition of the experiments that are later carried out, about Solar radiation, characteristics of the atmosphere that surrounds the Earth and photovoltaic cells.

- Then, the **second part** describes the procedure used to design the device that is going to be launched with the balloon along with the experiments done to characterize the solar cells and a theoretical study of the insulation and radiation filters that may be included to protect the array of cells.
- Lastly, the **third part** constitutes the conclusions and implementation on the high altitude balloon project as well as an costs analysis of the whole project.

2. SOLAR RADIATION

2.1. The Sun

The Sun is a star that constitutes the center of the Solar System. It is formed by hot gases, mainly hydrogen and helium. It was created 4.5 billions of years ago, when a nebula of gas and dust collapsed, due to gravitational forces. The Sun has a diameter of 1.39×10^9 m [2].

Besides, the Sun is considered a black body in scientific assumptions for easier calculations because the temperature of the outer layer can be approximated as 5777 K. However, it reaches around 8×10^6 K to 40×10^6 K at its center [3]. These elevated temperatures come from the nuclear fusion reactions that occur in the so called star. It is known as a proton-proton fusion and takes place in the core of the Sun. Following this, hydrogen nucleus (protons) collide and join together to form helium, which results in big releases of energy. This energy propagates through the layers of the Sun until it reaches the surface and part of it is radiated to the space [4]. The radiant flux is 3.8×10^{26} W, around 62.5 MW/m², from which only 1.37 kW/m² reaches the atmosphere of the Earth.

The Sun possesses six different layers (Fig. 2.1). Sorted from interior to exterior, the next parts are defined [5]:

1. **Core.** It has a radius of 150000 km approximately and it concentrates 40% of the total solar mass. Here the nuclear reactions of fusion that originate the energy of the star take place. It is constituted by many hydrogen atoms that are pushed together due to the gravitational forces. The atoms collide and, in some occasions, they fuse becoming helium and releasing energy.
2. **Radiative layer.** This layer goes until the 450000 km of radius. The density and pressure values are 10 times lower than in the core and the temperature decreases until 4×10^6 K. In this part, the energy released from the core is in the form of photons that try to pass outwards to the other layers of the Sun. The energy passes following a radiative process and it is very slow because of the collisions among them and with other particles.
3. **Convection layer.** It has a thickness of 250000 km and the average temperatures decrease to 6×10^5 K. In this layer, the energy is transmitted through convection. The colder gases contained inside the layer descend until reaching the surface of the previous layer where the photons heat them up. The gases expand and due to convection, the gases ascend to the outer layers of the Sun, that are at lower temperatures. The rises and falls of the gases originate convective currents.

4. **Photosphere.** This layer is the one that can be seen from Earth because it is where the light and heat generated by the nuclear reactions in the core are emitted to the space. It is thinner than the previous ones, less than 400 km and the temperatures are around 6000 K (black body assumption¹).
5. **Chromosphere.** This layer is constituted by hot gases and it can only be seen from the Earth during an eclipse. It has many magnetic fields that produce solar flares and sunspots and the elevated temperatures gives it the reddish color.
6. **Corona.** It is the outer layer of the Sun and constitutes the external part of the chromosphere. The temperatures reach almost 2 million K and it is formed by hot gases as well as the previous layers and the it extends from the end of the chromosphere and until more than a million of kilometers.

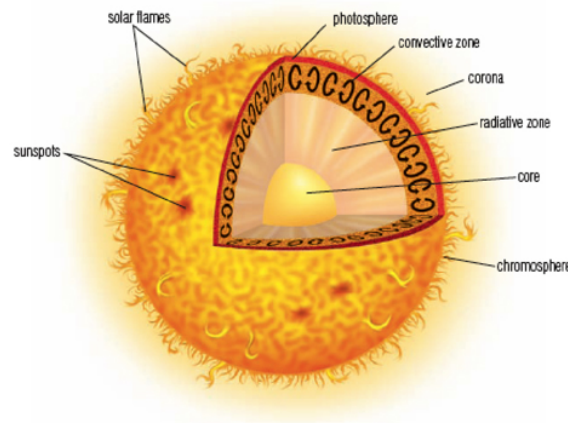


Fig. 2.1. Layers of the Sun

2.2. Radiation

Radiation is known as the energy that propagates through a medium or empty space. Therefore, the solar radiation is the energy released from the sun in the form of electromagnetic waves. The wavelength range of the solar spectrum goes from $0.27\ \mu\text{m}$ to $4.0\ \mu\text{m}$. Humans can only see radiation that is within the range from $0.4\ \mu\text{m}$ to $0.7\ \mu\text{m}$ and that explains how we can see the sunlight[3]. However, we are not able to appreciate the ultraviolet and infrared radiation that come from the Sun as well.

¹A black body is an ideal case which assumes a body that absorbs all the electromagnetic radiation incident on it [6]

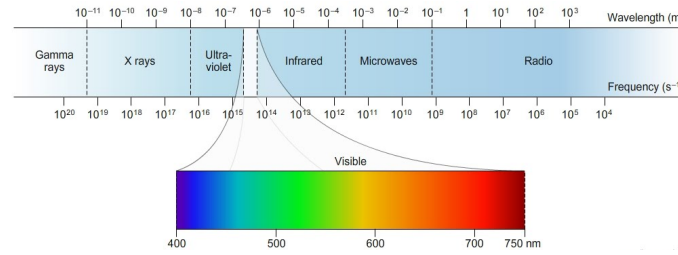


Fig. 2.2. Electromagnetic Spectrum [7]

Solar radiation is defined by the solar constant and the air mass zero solar spectral irradiance. The solar constant (G_{sc}) determines the “energy from the sun per unit time received on a unit area of surface perpendicular to the direction of propagation of the radiation at mean earth-sun distance outside the atmosphere” [8]. Its mean value is 1360 W/m^2 , though it changes slightly throughout the year, being at its maximum when the Earth is closest to the Sun, at the perihelion, due to the elliptical form of the Earth orbit around the Sun. The solar spectral irradiance is the distribution of this power density with respect to the wavelength, that is the radiation that would be received without the atmosphere. The curve shown in Figure 2.3 is based on measurements made by researchers at high altitude stations, aircrafts and satellites. 99% of the energy that comes from the Sun is located in the wavelength range from $0.27 \mu\text{m}$ to $4.0 \mu\text{m}$. In the case of solar cells, they are very sensitive to the spectral region between $0.4 \mu\text{m}$ to $1.1 \mu\text{m}$.

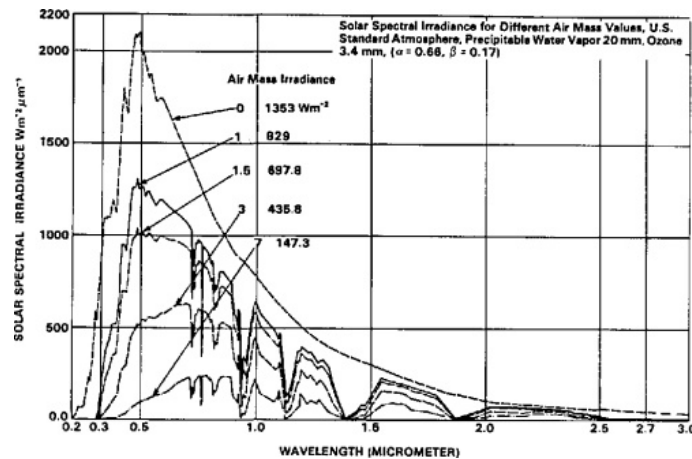


Fig. 2.3. Solar spectral irradiance [9]

However, when radiation coming from the Sun passes through the atmosphere layers, it attenuates, so the radiation that reaches the surface of the Earth is lower than 80% of the original radiation coming from the Sun. The solar radiation that comes directly from the Sun without being scattered is called **beam** radiation (G_b), while the radiation that comes from different directions due to scattering (scattered and reflected from other bodies) it is known as **diffuse** (G_d). Beam radiation can be concentrated while diffuse radiation cannot, most of the times, and the sum of both beam and diffuse is the total solar radiation (G). The part of solar radiation that does not reach the surface of the Earth due to the

atmosphere is classified as [3]:

- **Absorbed radiation.** Part of the radiation that disappears because it is taken in during its pass through the atmosphere. Among the main absorbers of radiation, there are the ozone (O_3), oxygen (O_2), clouds or greenhouse gases (such as H_2O , CO_2 , N_2O).
- **Scattered radiation.** Part of the Sun radiation that is deviated. Scattered radiation includes Rayleigh scattering, from particles that have a smaller diameter than $1/10^{th}$ of the wavelength of the incident radiation, and Mie scattering, from particles that have a diameter larger than the wavelength of the incident radiation.
- **Reflected radiation.** Part of the radiation that is returned by the object the electromagnetic wave falls upon either back to the space or to other surfaces or particles, differentiating the specular reflection, the wave is directed away in a single direction, and the diffuse reflection, where the incident radiation hits a not uniform surface and therefore the electromagnetic wave goes away in different directions. The reflected radiation constitutes $1/5$ of the total radiation.
- **Transmitted radiation.** Part of the electromagnetic radiation that passes through a medium. The direction of the electromagnetic wave changes when it penetrates the medium.

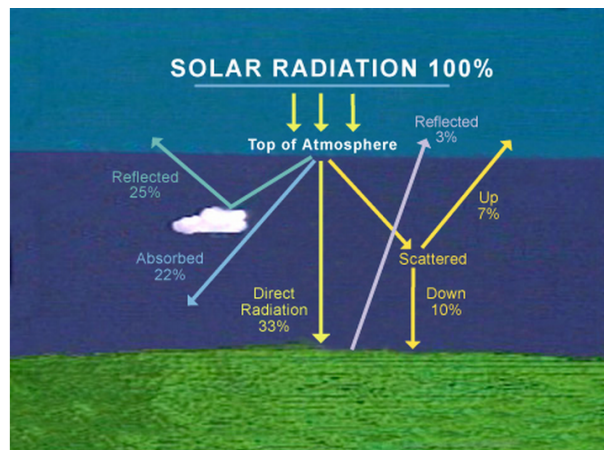


Fig. 2.4. Solar Radiation through the atmosphere [10]

As it has been explained, the atmosphere layers of the Earth avoid Sun radiation from hitting directly the surface of the Earth, making possible the existence of life. Also, Sun radiation changes with many other parameters, such as the day of the year, the hour of the day and the latitude and longitude of the location where the electromagnetic wave hits a surface.

2.3. The Earth-Sun relations

It is well known that the Earth has two main movements: translation and rotation. Firstly, rotation is the movement of the globe around its axis from West to East, completing a turn every 23 hours and 56 minutes, almost the 24 hours that define a day. The axis of rotation is tilted 23.45° of the plane of the orbit the Earth describes around the Sun. Secondly, the changing in position in the orbit path is called translation. The Earth takes 365 days, 5 hours, 45 minutes and 46 seconds to complete a turn around the Sun, defining what it is called a year.

Besides, these movements and the inclination of the axis of rotation define the seasons throughout the year. The four seasons end and begin during the solstices and equinoxes. In one hand, the solstice is the moment when the Sun is at its furthest point North or South the Equator and therefore the day has the longest hours of day, during the Summer solstice of the Northern hemisphere around the 21st of June, or night, in the Winter solstice of the Northern hemisphere the 21st of December. On the other hand, the equinox is the moment when the Sun is aligned with the Equator plane and the hours of day and night are the same. This occurs twice over the year, on the 20th of March in the upper hemisphere, the Spring equinox, and the Autumn equinox, around the 22nd of September.

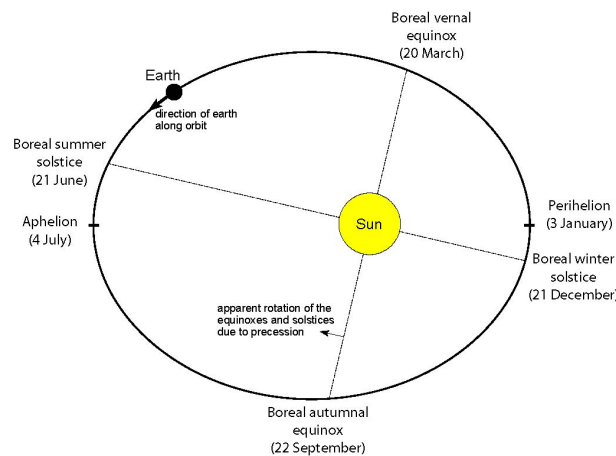


Fig. 2.5. Solstices and Equinoxes [11]

On the contrary, in the Southern hemisphere, the Summer and Winter solstices as well as both equinoxes occur in opposite order. Additionally, the point where the Earth is the closest to the Sun is the Perihelion, during the 3rd of January, and the point at its furthest is called the aphelion, occurring at the 4th of July [12].

2.3.1. Radius Earth-Sun estimation

The average distance from the Earth (R_o) is 1.49×10^{11} m which is one Astronomical Unit. The Earth makes an elliptical path around the Sun, with an eccentricity of 0.0167, and this distance Sun to Earth changes through the year. The gap (R) can be calculated

with Eq. 2.1 and Eq. 2.2, where d is the day number of the year and R_c the vector radius correction term [13].

$$R_c = 1 + 0.033 \cdot \cos\left(\frac{360 \cdot d}{365}\right) \quad (2.1)$$

$$R_c = \left(\frac{R_o}{R}\right)^2 \quad (2.2)$$

Nevertheless, these formulas allow to obtain an approximated value of the distance between the Sun and the Earth and they are a simplification, following Kepler's Second law, where he states that "the line connecting the Sun to a planet sweeps equal areas in equal times"[14]. The most characteristic radii are the largest (aphelion), which is 1.53×10^{11} meters, and the shortest (perihelion) whose value is 1.48×10^{11} meters.

2.3.2. Variations in Extraterrestrial radiation

The extraterrestrial radiation that enters the atmosphere changes depending on the day number of the year, being at its maximum at the perihelion and at its minimum at the aphelion.

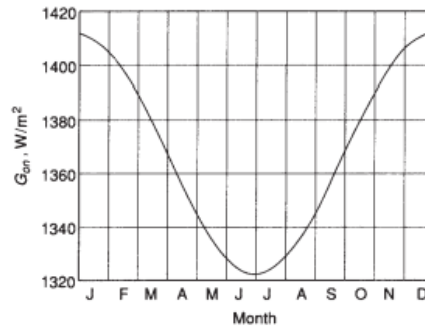


Fig. 2.6. Variation of G_{on} through the year [3]

The extraterrestrial radiation (G_{on}) incident on a plane normal to the radiation (Equation 2.3) on the day of the year needed can be calculated. Basically, the extraterrestrial radiation on a normal plane is the solar constant (G_{sc}) modified by the vector radius correction term (R_c).

$$G_{on} = G_{sc} \cdot \left[1 + 0.033 \cdot \cos\left(\frac{360 \cdot d}{365}\right) \right] \quad (2.3)$$

Then, the extraterrestrial radiation on a horizontal plane, parallel to the surface horizontal reference surface, with θ as the incidence angle:

$$G_o = G_{on} \cdot \cos(\theta) \quad (W/m^2) \quad (2.4)$$

Then, the daily extraterrestrial irradiance is obtained by integrating G_o over the daylight hours, obtaining (H_o) in kJ/m^2 .

$$H_0 = \frac{24 \cdot 3600 \cdot G_{\text{on}}}{\pi} \cdot \left[\cos(L) \cos(\delta) \sin(H_{\text{sunset}}) + \sin(L) \sin(\delta) \cdot \frac{H_{\text{sunset}} \cdot \pi}{180} \right] \quad (2.5)$$

Lastly, the hourly extraterrestrial irradiance I_0 on a horizontal surface:

$$I_o = \frac{12 \cdot 3600 \cdot G_{on}}{\pi} \cdot \left[\cos(L)\cos(\delta)\sin(H_b - H_a) + \sin(L)\sin(\delta) \cdot \frac{(H_b - H_a) \cdot \pi}{180} \right] \quad (2.6)$$

2.3.3. Solar Angles

In order to describe the position of the Sun relative to a surface, the characteristic angles and geometric relationships between the incident surface, the Sun and the Earth need to be defined.

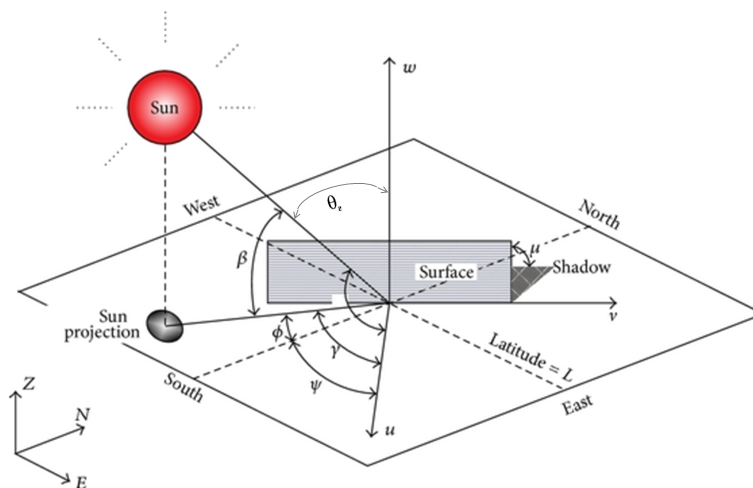


Fig. 2.7. Solar Angles

The angles are the following [3]:

Declination (δ) This angle is related to the tilting of the Earth's rotation axis with respect to the plane that contains the orbit of the Earth around the Sun. It is the angle between the plane formed by the Equator and the plane formed by the Earth's orbit.

$$\delta = 23.45^\circ \cdot \sin \left[360 \cdot \left(\frac{d + 284}{365} \right) \right] \quad (2.7)$$

The values of the declination angle go from -23.45° to 23.45° , being at the maximum and minimum values during the Summer and Winter solstices. Moreover, the other value that stands out is when the declination angle is 0° , which happens during the Spring and Autumn equinoxes and explains the equal number of hours of day and night.

Hour (H) This is the angular displacement between the meridian where the surface is placed and the position of the Sun, East or West. It can be expressed in hours or in degrees where one hour is equivalent to 15° . The Equation 2.8 allows us to calculate its value in degrees knowing the solar time (2.12).

$$H = (ST - 12) \cdot 15 \quad (2.8)$$

Latitude (L) It is the angle that describes the position with respect to the Equator, North or South, and depends on the location where the surface is placed. The values go from -90° , at the South Pole, to 90° , at the North Pole.

Solar Altitude (β) It is the angle formed by the imaginary line joining the Sun and the surface and the horizontal plane on the Earth's surface.

Zenith (θ_z) It is the angular displacement between the Sun rays and the normal to the horizontal surface.

The zenith and the solar altitude angles are complementary angles and thus the addition of them is 90° . Equation 2.9 allows the calculation of θ_z and β by establishing a relationship among the latitude, the declination angle and the hour angle.

$$\sin(\beta) = \cos(\theta_z) = \sin(L) \cdot \sin(\delta) + \cos(L) \cdot \cos(\delta) \cdot \cos(h) \quad (2.9)$$

Solar Azimuth (ϕ) Angle constituted by the projection of the sun rays on the horizontal plane and the reference line for South. If the angle goes from the South to East, if the value is negative and if the displacement goes West, it is positive.

$$\sin(\phi) = \frac{\cos(\delta) \cdot \sin(H)}{\cos(\beta)} \quad (2.10)$$

Surface-solar Azimuth (γ) This angle goes from the projection of the line to the Sun and to the projection of the normal to the surface. It is a relation within the Surface Azimuth and the Solar Azimuth angles.

Surface Azimuth (ψ) It is the angle formed by the projection of the normal to the surface with reference line for South on the horizontal plane. The values of this angle go from -180° to 180° , being 0° at South, negative to the East and positive to the West.

Slope (μ) It is the inclination of the surface where the Sun rays fall upon with respect to the horizontal plane.

Incidence (θ) In contrast to the Zenith angle, this is the deviation from the line to the Sun and the normal to the surface.

$$\begin{aligned} \cos(\theta) = & \sin(L)\sin(\delta)\cos(\mu) - \\ & \cos(L)\sin(\delta)\sin(\mu)\cos(\psi) + \\ & \cos(L)\cos(\delta)\cos(H)\sin(\mu)\cos(\psi) + \\ & \cos(\delta)\sin(H)\sin(\mu)\sin(\psi) \end{aligned} \quad (2.11)$$

2.3.4. Solar Time

The time when the Sun crosses the local meridian, that is when the Sun is at its maximum point in the sky during the day, the so called solar time (ST), and the time when the clock strikes twelve o'clock in the morning, the local time (LT) need to be differentiated. The Earth is divided in 24 equal sections of approximately 15° , the time zones. The reference imaginary line for this standard time is the meridian of Greenwich, for time zone 0.

The criteria followed is the numbering of the zones, positive to the East and negative to the West. By knowing the local time, the solar time can be calculated by making three corrections. Firstly, the difference the local meridian (L_{st}) and the meridian on which the local time is based (L_{loc}). Secondly, the equation of time (E), which is the time the Earth takes to do the same distances along its orbit and it is calculated with Equation 2.13 and Equation 2.14, where d is the day number of the year.

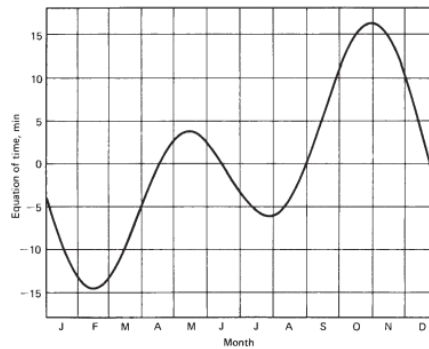


Fig. 2.8. Equation of time throughout the year [3]

Lastly, the daylight saving (DS), which is the method used in order to take advantage of the most daylight hours of a day. Clocks are advanced one hour during Summer and delayed one hour during the Winter. The daylight saving value is 0 during the Winter time and 60 minutes during the Summer time. Considering all of these corrections, the solar time is calculated following the Equation 2.12.

$$ST = LT + 4(L_{st} - L_{loc}) + E - DS \quad (2.12)$$

$$E_t = 9.87 \cdot \sin(2B) - 7.53 \cos(B) - 1.5 \cdot \sin(B) \quad (2.13)$$

$$B = \frac{(d - 81) \cdot 360}{364} \quad (2.14)$$

2.3.5. Clearness Index

This index refers to the transparency of the atmosphere and the amount of solar radiation that can pass through it. It establishes a relationship between the extraterrestrial radiation coming from the Sun before going through the atmosphere and the radiation that hits the surface of the Earth after crossing the atmosphere. Three clearness indexes can be calculated [13].

Firstly, the hourly clearness index which is the ratio between the hourly total radiation on a horizontal surface and the hourly extraterrestrial irradiance (Eq 2.15). Secondly, the daily clearness index, which compares the daily total radiation on a horizontal surface and the daily extraterrestrial irradiance (Eq 2.16). Lastly, the monthly average clearness index for the ratio between the total monthly average radiation and the monthly average extraterrestrial irradiance (Eq 2.17).

$$k_t = \frac{I}{I_o} \quad (2.15)$$

$$K_t = \frac{H}{H_o} \quad (2.16)$$

$$\bar{K}_t = \frac{\bar{H}}{\bar{H}_o} \quad (2.17)$$

2.3.6. Albedo

As it has been explained in Section 2.2, when solar radiation hits the ground, part of it is reflected. The albedo is the ratio that compares the radiation reflected from the surface to the radiation that initially fell upon the surface. It is expressed as a percentage and the common albedo of the ground is that of 20%, higher when the ground is brighter and lower when it is darker. The albedo is taken into account in diffuse radiation as the reflected ray goes back to the sky, where it is scattered.

3. THE EARTH ATMOSPHERE

The atmosphere is the combination of layers that surround the Earth. These layers are mainly made by stable gases spread out in different proportions depending on the altitude, some liquids and solids such as ashes, ice, pollen and other small floating particles, and stuck together due to the gravitational force and gas compressibility. It covers the Earth from its surface and up to 10,000 km, however, 95% of its mass is concentrated in the first 15 km.

Moreover, the atmosphere fulfills two main functions that allow the Earth suitable for life: protection and regulation. Firstly, the protective function as the atmosphere acts as a natural filter of the radiation coming from the Sun absorbing most part of it. In the Ionosphere (Section 3.2), the upper layer of the atmosphere, shortwave radiation are absorbed; the ozone layer filters the ultraviolet radiation and finally, the CO₂ and water vapor suspended in the lower layers of the atmosphere, absorb part of the infrared radiation.

Secondly, the regulatory function, affects the temperatures and, consequently, the climate. Part of the reflected radiation in the Earth surface (albedo Subsection 2.3.6) is absorbed by the atmosphere, forbidding temperatures to rise exponentially; then the greenhouse effect, produced by the reflection of the radiation that comes from the Earth back to Earth by the gases of the atmosphere, warming it up and avoiding temperatures to abruptly go down; at last, the circulation of the air from top to bottom of the atmosphere, due to density variations, allows the temperatures to be maintained without significant changes.

3.1. Chemical composition of the atmosphere

In the atmosphere, two main parts can be differentiated, depending on the chemical composition of the air. The first part, that goes from the Earth surface until 90 km up, has an homogeneous distribution of gases and thus is called the homosphere [15].

Homosphere	
Component	Percentage
N ₂	78.083%
O	20.945%
Ar	0.934%
CO ₂	0.035%
Water vapor	1-4%

Table 3.1. Main components of the homosphere

From this altitude the concentration of gases has a much more higher variability and the

predominant gas depends on the altitude, therefore this second part is called the heterosphere. In Table 3.2 [15], each component is represented along with the altitude range where it is the main element [16].

Heterosphere	
Component	Altitude
N ₂	100-200 km
O	200-1,000 km
He	1,000-3,500 km
H	<3,500 km

Table 3.2. Main components of the heterosphere

Apart from the gases, the atmosphere is also filled with aerosols, colloidal suspension in the gases of the atmosphere of liquids and solids (mainly dust and water vapor) with sizes between 1 to 200 μm .

3.2. Layers of the atmosphere

Depending on the altitude and the composition, the homosphere is divided in the troposphere, stratosphere, mesosphere and, in the other hand, the heterosphere is constituted by the thermosphere and the exosphere [15].

The first layer, starting from the Earth surface, also called the planetary boundary layer or PBL, and until 10 kilometers high (the altitude of the troposphere higher in the Equator and lower in the poles due to the shape of the Earth's crust), is the troposphere. In this part, more than 70% of the mass of the atmosphere is concentrated. The PBL is heated up by the Sun radiation and it warms up the air, which ascends while decreasing its temperature. This phenomena is the basis of the air circulation in the atmosphere, allowing water vapor, particles and pollutants to move, and acting as a temperature regulator. Additionally, water vapor and CO₂ favor the greenhouse effect. After the troposphere, there is an extension of the atmosphere where the temperature remains almost constant and divides the troposphere from the stratosphere. It is called the tropopause and the altitude of this layer depends on the weather, being at a higher altitude in warm climates and lower in colder parts of the Earth, due to meteorological conditions, such as temperature, pressure and humidity, the Earth rotation, that creates air currents, and gravity. The tropopause avoids vertical currents of air to go from the troposphere to the stratosphere, blocking water vapor and particles to go higher to other atmosphere layers.

Afterwards, the stratosphere, which extension goes from the end of the tropopause at an average altitude of 20 kilometers and until 50 kilometers high, where the mesosphere starts. The stratosphere is constituted mainly by gases. The amount of water vapor is very low as the tropopause does not allow the pass of it. Due to the high concentration of

ozone, that absorbs almost all the ultraviolet radiation coming from the Sun, in this part, the temperature gradient changes with respect to the troposphere, and temperature starts increasing (temperature inversion), until reaching a value near 0°C. The concentration of ozone in the stratosphere peaks from 20 to 25 kilometers, and this occurs because of the photodissociation, by which the oxygen interacts with high-energy photons resulting ozone. In the stratosphere there is no vertical circulation of the air, but there are horizontal gusts of wind, known as jet streams, that can reach 200 km/h.

Then, there is another thin layer called stratopause, where temperature does not change with altitude. Following this layer, there is the mesosphere, the last part of the atmosphere where the gases are mixed up (homosphere). Its altitude reaches 85 kilometers from the PBL. In this layer, most of the meteors burn due to the gases that constitute it and works as a barrier, preventing celestial bodies to hit the Earth surface. Because of this, the concentration of iron and other metal elements is relatively higher in this layer than in others. The temperature decreases again with altitude, as in the troposphere reaching the coldest temperatures of the atmosphere (less than -90°C). In the mesosphere takes place the phenomena of the noctilucent or polar mesospheric clouds, which are compressed ice crystal clouds that show reflections of light that can occasionally be seen from the polar caps, due to the scattering of sunlight in the crystals that form the clouds. The mesosphere ends with the mesopause, another layer, thicker than the other layers with constant temperature, that separates the mesosphere from the thermosphere.

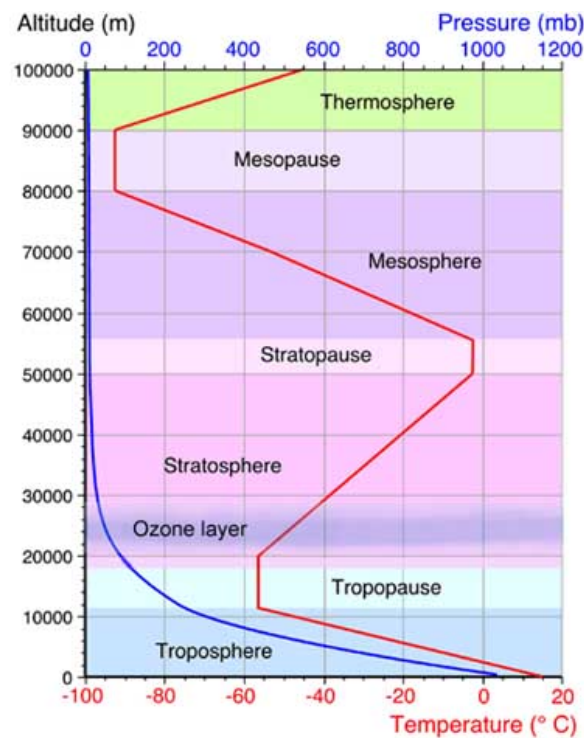


Fig. 3.1. Atmosphere layers and temperature gradient [17]

Subsequently, the gas concentration of the layers is not homogeneous anymore and the

thermosphere starts with the thermosphere. The main components of the air are the atomic oxygen, atomic nitrogen and helium and the density is very low. Here, a temperature inversion takes place as well as in the stratosphere, temperature increases with altitude up to 1,000-1,500°C, because most of the ultraviolet and x-rays are absorbed in this layer. Its extension goes from 90 kilometers to 500-1,000 kilometers high, making it the thickest layer of the atmosphere. However, it is considered that the atmosphere only reaches 100 kilometers, as the constitution of the layers above this altitude is very similar to the outer space characteristics. Additionally, the thermosphere contains the ionosphere, a very thin layer where the energy of the photons coming from Sun radiation is very high and ionizes the molecules, taking away their electrons, creating ions. The collisions between these ions produce the Northern and Southern lights that can be seen from regions near the polar caps in the Earth surface. In the thermopause, the International Space Station orbits around the Earth.

Lastly, the exosphere. It is separated from the thermosphere by the thermopause, placed at around 800 kilometers high from the Earth's crust. The exosphere is the outer shell of the atmosphere and its altitude goes up until 10,000 kilometers. It represents the transit from the Earth's atmosphere to the outer space. The exosphere is mainly constituted by plasma. Also, the air density in this particular layer is almost zero and the concept of temperature is measured by the speed of the atoms, being hotter when the speed is higher.

Apart from temperature, the pressure also changes with altitude. It decreases exponentially, from 1 atmosphere at the surface of the Earth, until achieving an almost zero value in the stratosphere. Furthermore, the density of the air decreases with altitude as well, due to the gravitational forces.

4. PHOTOVOLTAIC CELLS

In the following chapter, the functioning of solar cells is explained. Starting from the photoelectric effect, whose discovery allowed the development of the cells and the exploitation of solar energy, it covers the composition, structure and parameters of the photovoltaic cells. Understanding well the operation of the cells will be the key in the choosing of the optimum solar cells for the project.

4.1. The photoelectric effect

In 1887, Heinrich Hertz discovered the photoelectric effect [18], while trying to prove the electromagnetic wave behavior of the light described by Maxwell in his equations. This accidental discovery made him doubt about the theory of the light about the light being an electromagnetic wave; while illuminating a metallic ball and moving it closer to another ball, the electrical discharge that occurred between them increased. He investigated this unexpected effect during months but he could not reach any conclusion or formulate any theory that explained the phenomenon.

Two years later, Thomson found out that the particles emitted during this effect were electrons. Lately, Philipp Lenard, made experiments to see the change in the energy of the electrons increasing and decreasing the frequency of the light that was incident on the metallic ball.

In 1905, Albert Einstein won the Nobel Prize in Physics due to his article about the photoelectric effect. In his experiment, Einstein developed a circuit connected to an evacuated chamber. Incident radiation enters the chamber and into a metal surface, the cathode, causing electrons to be emitted and some of them reach an opposing metal surface, the anode, creating an electric current between the metal plates. The response of the electrons to the light is the photoelectric effect [19].

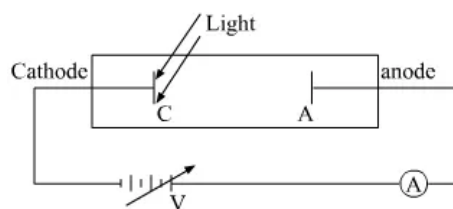


Fig. 4.1. Apparatus photoelectric effect [20]

Einstein proved that the maximum kinetic energy of the emitted electrons was independent of the intensity of the incident radiation. The intensity of a light beam is the power per unit area, which is the number of photons per unit area per unit time and multiplied

by the energy per photon. The photons of the light beam collide with the electrons of the metal surface, giving all their energy to the electrons.

By increasing the incident light, a rise in the energy absorbed by the electrons and, therefore, a growing kinetic energy would be expected. However, the experiments performed by Einstein showed that the maximum kinetic energy was the same for each wavelength, no matter the intensity of that radiation. Changing the intensity would lead to the increase of the quantity of electrons emitted from the metal, not the kinetic energy.

This experiment proves the particle-like behavior of the light. Additionally, the light particles are called photons, whose energy is described in the Einstein equation 4.1 for photon energy [21]. It shows that the energy of a photon is given by the frequency of the light and Planck's constant ($h = 6.626 \times 10^{-34} \text{ J s}$).

$$E = hf = \frac{hc}{\lambda} \quad (4.1)$$

Therefore, as the frequency of the electromagnetic wave increases, the energy of photons increases. Consequently, when the wavelength is shorter, the energy is higher, as the wavelength is the inverse of the frequency. The photoelectric effect makes possible the functioning of a solar cell through the photovoltaic effect.

4.2. Composition of PV cells

A solar cell is a device, formed by semiconductor materials, that transforms the energy that comes from Sun radiation into electricity. Solar cells can have different shapes and sizes.

A semiconductor material is composed out of chemical elements spread out in different periodic table groups and its characteristics depend on the atomic number of the element [22]. Moreover, a semiconductor material can be composed by one or more elements. In one hand, the most common elements are the silicon (Si), used in more than 90% of the production of solar cells, and the Germanium; and in the other hand, the compounds more used are the GaAs, the PIn and the AsGaAl.

These materials have both metal elements characteristics, they allow the current flow, and insulators characteristics, depending on the external conditions the materials are subjected to, such as temperature or pressure variations, being exposed to a magnetic or an electric field, or an incident radiation.

Furthermore, semiconductor materials are constituted by an array of atoms joined together with covalent bonds, forming a structure that repeats itself [23]. For example, in the case of Silicon, which has four electrons in the outer shell of the atom, forms four covalent bonds with another four Silicon atoms. This way, the Silicon is getting the eight electrons in the valence shell needed to reach stability, creating a lattice.

As the temperature increases, the electrons that form the covalent bonds in the lattice

of the semiconductor material reach a higher energy level and break away from their bonds, becoming free electrons. The flow of these electrons to holes left by other free electrons means the current is passing through the material and it behaves like a conductor, although it has not conductive properties as good as a metal. These energy levels can be reached at ambient temperature. However, at low temperatures, the electrons of the covalent bonds cannot increase their energy enough to move freely and they are stuck in the bonds. In this case, the material acts as an insulator. The minimum energy level that an electron in a covalent bond must get to become a free electron is the band gap (E_g). In photovoltaics, the band gap is reached through the photoelectric effect (Section 4.1). The incident photons with an energy level equal or higher than the band gap are absorbed by the semiconductor materials, the electrons are pushed out of the covalent bond creating a hole, which will be later occupied by another free electron, and the energy of the photon is released.

Semiconductors can be pure or modified (doped) in order to increase their conductivity. Depending on the level of purity, there exist two types of semiconductor materials. Ones are called intrinsic semiconductors and they allow the flow of current without being modified, they are completely pure. But the other type, which are called extrinsic semiconductors, are added an amount of impurities that changes the electrical conductivity of the material. The process in which impurities are added to an intrinsic semiconductor, in order to make it extrinsic and alter its characteristics, is doping. Depending on the doping process, two kind of extrinsic semiconductors are found [23]:

- **N-type semiconductors**, which consist of increasing the number of free electrons of the material (negatively charged). They are constituted by elements from group IV of the periodic table doped with elements from group V. As they have five electrons in the valence shell, this impurities are known as pentavalent impurities. Also, this dopant atoms are called donors as they "give" electrons to the original semiconductor.
- **P-type semiconductors**, which are doped by increasing the number of holes (material with positive charge) and they are elements from IV doped with elements on group III, so that they are known as trivalent impurities. These kind of dopants are called acceptor as they increase the number of holes in the lattice of the semiconductor that is being modified.

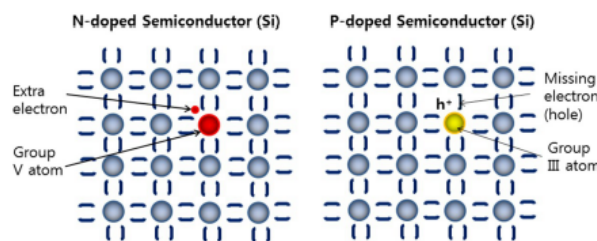


Fig. 4.2. N-type and P-type semiconductor materials [23]

A solar cell is constituted by the union of a n-type semiconductor with a p-type. The junction of the edges of the semiconductors is called the depletion or diffusion zone. When these two types of semiconductors are joined together, the free electrons of the n-type go to fill the holes of the p-type semiconductor, forming a p-n junction. Before combining the two types together, they have neutral charge. When they are linked, as the holes of the p-type are occupied with electrons, the semiconductor becomes an anion (negatively charged) and, in the case of the n-type, as electrons diffuse to the holes in the p-type, it becomes a cation (positively charged); creating an electric field. Consequently, a potential difference appears between the two semiconductors (photovoltaic effect). If the solar cell is connected to an external load, the current will flow through it from the p-type to the n-type.

4.3. Characteristic parameters of a PV cell

Furthermore, a solar cell behaves like a diode, allowing the flow of current when radiation falls upon it and avoiding the flow when there is no sunlight. In Figure 4.3, the equivalent circuit of a solar cell is represented. Firstly, I_L is the current generated by the photovoltaic effect.

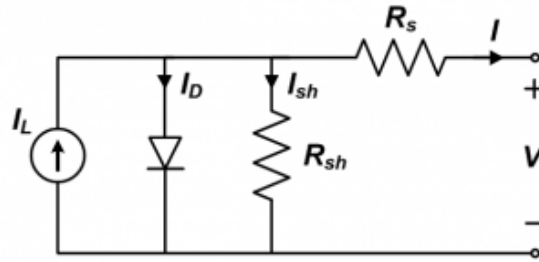


Fig. 4.3. Equivalent circuit of a solar cell

Secondly, I_D , defines the diode current. It depends on the dark saturation current (I_0) and follows the Shockley equation for an ideal diode (Equation 4.2), where q is the electron charge (1.602×10^{-19} J/V), k the Boltzmann's constant (1.3806×10^{-23} J/V) and T_c the cell temperature.

$$I_D = I_0 \cdot \left[\exp\left(\frac{q \cdot V}{k \cdot T_c}\right) - 1 \right] \quad (4.2)$$

Thirdly, the resistance in parallel to the diode, the shunt resistance (R_{sh}), are the losses due to impurities in the semiconductor or in the junction of both of them and has a high value. Then, the series resistance (R_s), which stands for the losses due to connections and its value is typically low. Finally, I and V which are the current and voltage, respectively, supplied by the solar cell.

Consequently, applying Kirchhoff laws on the circuit in Figure 4.3:

$$I_L = I_D + I_{sh} + I \quad (4.3)$$

Then, solving for the current:

$$I = I_L - I_D - I_{sh} \quad (4.4)$$

Finally, substituting the previous expressions:

$$I = I_L - I_0 \cdot \left[\exp\left(\frac{q \cdot V}{k \cdot T_c}\right) - 1 \right] - \frac{V + IR_s}{R_{sh}} \quad (4.5)$$

However, this equation can be simplified assuming that the value of the shunt resistance is very large and then the I_{sh} is rounded to zero, leaving the correlation between current and voltage as:

$$I = I_L - I_0 \cdot \left[\exp\left(\frac{q \cdot V}{k \cdot T_c}\right) - 1 \right] \quad (4.6)$$

From this expression, the characteristic parameters of a solar cell are defined. In the first place, the short circuit current (I_{sc}). It is the maximum current of a solar cell at a certain radiation level and temperature and it is measured when the voltage across the cell is 0, when the cell is short-circuited. Then, the open circuit voltage (V_{oc}), which is the maximum voltage of the solar cell, that is when the current is null. Additionally, the open circuit voltage decreases when the temperature of the cell increases [24] and the short circuit current shifts significantly with solar radiation, increasing when radiation gets higher [25].

Besides, the power can be calculated by the multiplication of the voltage and the current. The maximum power is obtained by multiplying V_{oc} and I_{sc} with the fill factor (FF) [26]. This factor defines the quality of a solar cell.

$$P_{max} = V_{oc} \cdot I_{sc} \cdot FF \quad (4.7)$$

Additionally, the maximum power can be obtained with the maximum voltage and current. This point is the MPPT (Maximum Power Point Tracking). Lastly, the efficiency of

a solar cell is given by the maximum power, the incident radiation and the area of the cell.

$$\eta_{\max} = \frac{P_{\max}}{A_{\text{cell}} \cdot G} \quad (4.8)$$

Also, these values will change if two cells or more are connected to each other. If the cells are connected in series, the total voltage is the voltage of an individual solar cell times the number of cells in the array, the current remaining constant. On the contrary, if the cells are connected in parallel, the voltage is the same while the current is the the current flowing through an individual solar cell times the number of cells in parallel.

From the parameters described before, the characteristic I-V curve is obtained:

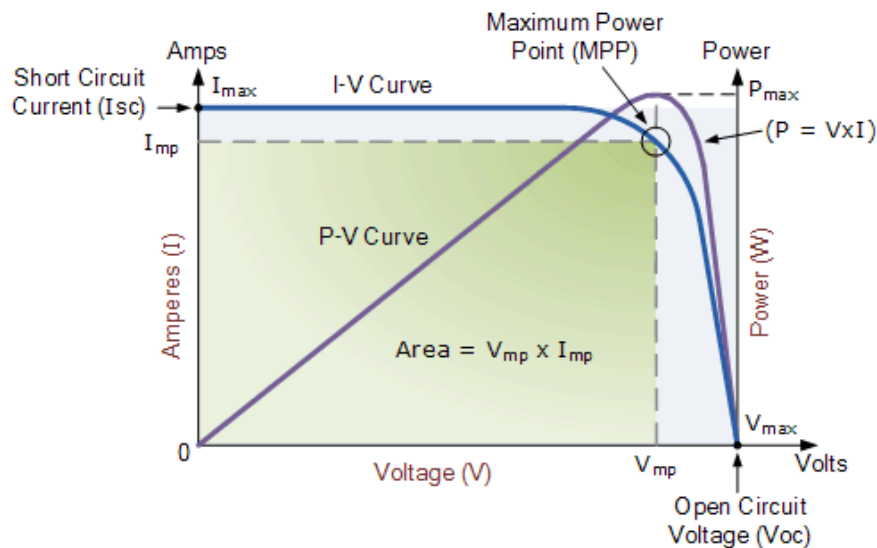


Fig. 4.4. I-V curve of a solar cell [27]

4.4. Types of PV cells

Depending on the manufacturing process, photovoltaic cells are classified in the following types [28]:

- **Monocrystalline.** These type of solar cells are made of silicon. It has been used since the development of the first cells. The processing of the silicon is expensive, difficult, slow and requires a high energy use. However, it is the most efficient type, 15 to 20% and have better performance than other kinds of cells at low radiation conditions.
- **Polycrystalline.** In contrast with the monocrystalline silicon, the process of developing polycrystalline is less expensive, faster and with low energy costs. Neverthe-

less, the typical efficiency range is lower, 13 to 16%, and the temperature tolerance range is also smaller.

- **Amorphous.** It is also known as thin-film solar cell. They have the cheapest costs of all the cell types. It is made by creating a thin silicon layer over a glass substrate and covered by a conductor material layer.

Besides, they are not as brittle as the previous types and they are more flexible, thus the assembly is easier.

However, the level of impurities in the silicon, decreases the performance of the cell. Also, amorphous cells can be made out of other semiconductor materials, like CuInSe_2 or CdS . The typical efficiency of these kind of cells oscillates between 14 to 15%.

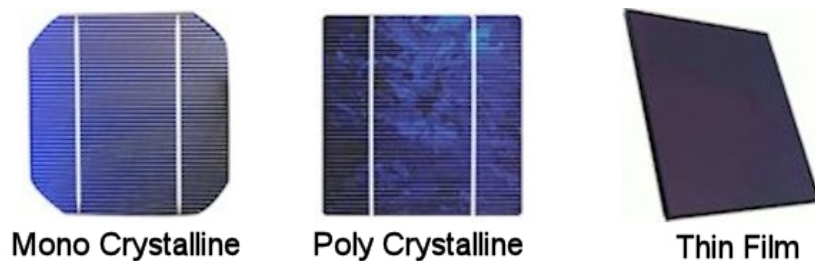


Fig. 4.5. Monocrystalline, Polycrystalline and Amorphous solar cells [29]

Furthermore, photovoltaic cells can be classified in generations over their history. The first generation solar cells include the monocrystalline and polycrystalline silicon solar cells. They were the first to be developed, during the 1950s and they are characterized by large areas, high quality, efficiency and durability, and a single junction between the semiconductors.

As the prices needed to be more competitive, the second generation of solar cells appeared. Here, the thin-film type is found. These cells have been made to decrease the costs and energy waste. The silicon is replaced by other materials such as the copper indium gallium selenide (CuInSe), usually referred as CIGS, and the cadmium telluride (CdTe).

Lastly, the third generation of solar cells is currently under investigation. They stand out due to having the highest conversion efficiencies. While in the first and second generation the maximum performance achieved is around 25%, according to an article presented by the Special Research Centre for Third Generation Photovoltaics of the University of New South Wales in Australia [30], the theoretical efficiency of this generation is from 30 to 60%. That means more than half of the radiation coming from the sun could be used, making solar energy very competitive inside the energy market.

Amongst the types that are being developed and or under research, the article highlights the tandem cells and multiple electron-hole pairs. The tandem cells are based on the superposition of different band gaps in a cell so that more energy from the incident photons can be used and the multiple-electron hole pairs is based on taking advantage of the excess of energy in a cell, instead of being converted into heat, use it to develop more electron-hole pairs.

Additionally, the article describes three types that are only theoretical and currently under research. These are the hot carrier cells, which consist in reducing the energy losses when the solar cells cools after the photon has released its energy [31], multiband cells, based on the addition of a third band (impurity band) to the existing conduction and valence bands, and, finally, the thermophotovoltaic devices, where electricity is generated from heat through photons.

5. DEVICE SELECTION AND IMPLEMENTATION

In this chapter, the criteria followed in order to choose the solar cells needed to perform the experiments and that later will be attached to the high altitude balloon and launched to the stratosphere is described.

Moreover, the process of assembly of the solar cells to get the desired power is explained in detail. Also, the circuit designed to measure voltage and current and the Arduino code implemented to display the value of the parameters. Finally, all the data is going to be saved using a structure in Matlab.

5.1. Solar Cells Selection

The first thing that needs to be decided is the solar cells that are going to be bought. The criteria followed for the choosing of the cells is the following:

- **Temperature range** range that the PV cells can withstand. The balloon is going to fly from the surface of the Earth, in Madrid, until reaching the stratosphere, 30 km high. The altitude of Madrid is 640 m over the sea level. The balloon is launched during June and the average temperature of this month is 20 degrees Celsius [32].

According to Figure 3.1, it can be seen that the balloon, and thus the box with the cells, will ascend from the surface to the stratosphere, passing the troposphere, the tropopause and a great part of the stratosphere, depending on when the balloon bursts.

It can also be seen that the temperature range will go from almost -60°C to around $+20^{\circ}\text{C}$. Additionally, it has to be taken into account that the box may increase its temperature during the fall. However, finding a PV cell that can withstand these temperature variations could be almost impossible and very expensive. The solution is to study the different types of insulations used by devices that have to withstand similar temperature ranges and add the one that suits the most the requests of this particular project. The insulation of the solar cells is covered in Chapter 9.

- **Radiation range.** As the balloon rises, the radiation incident on the solar cells is higher. Whether the use of radiation filters will be needed or not has to be discussed.
- **Size** of the PV cells. Assuming that the box is 50 cm wide, long and height, the size of each cell must fit inside the square of side 50 cm. Cells with a maximum side measure of 25 cm will be considered so they have a wide tolerance with respect to the edges of the box.
- **Type.** Solar cells can be monocrystalline, polycrystalline, hybrid or amorphous. The more reliable and efficient type at these altitudes needs to be chosen.

- **Power** of the PV cell. The power has to be between 1 to 3 W, so the array of solar cells is small enough to fit on the box of the high altitude balloon and still gets significant voltage and current values.

Furthermore, something that needs to be taken into account is the manufacturer and sellers reliability.

After considering all the described criteria, the solar cells have been ordered to the Italian company Mr. Watt [33]. This particular company has been chosen because solar cells are sold by units and the ones with the characteristics that fulfill the purposes of the project can be easily selected. Also, it has been decided to buy monocrystalline solar cells due to the high efficiency and durability. The technical specifications of the solar cells are described in Table 5.1 and it is provided by the Mr. Watt company.

DATA SHEET	
Type	Monocrystalline
Height	63 mm
Width	63 mm
Thickness	9.84 mm
Weight	56.7 g
Power	0.7 W
Voltage	0.55 V
Current	1.4 A

Table 5.1. Technical specifications of a solar cell [33]

The voltage, current and power provided are calculated at a radiation of 1000 W/m^2 and these are the values at the maximum power point tracking (MPPT). In order to reach the desired power, it has been decided to create an array of four solar cells in series. Using the Matlab code, explained in Chapter 6, and assuming the specified values of Table 5.1, the approximation of the maximum efficiency of a solar cell is obtained, obtaining almost 19% and the characteristic I-V curve (Fig. 5.1).

The curve of the current versus the voltage, in Volts and Amperes respectively, and the power curve, expressed in Watts, are shown and it can be noted that the point of maximum efficiency matches the point of maximum power.

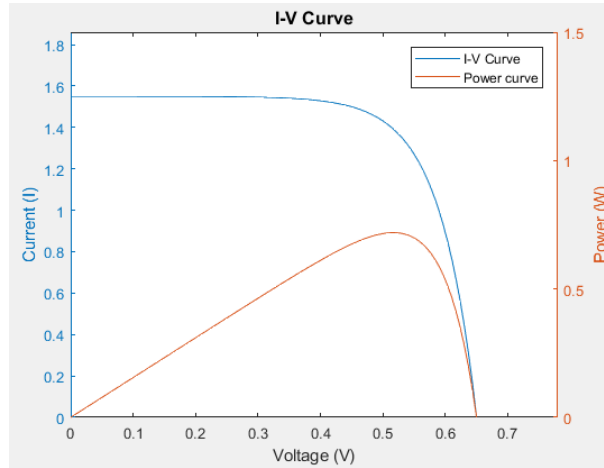


Fig. 5.1. I-V curve of one Mr. Watt solar cell

In order to compute the curve, a short circuit current of 1.5A and an open circuit voltage of 0.6V have been assumed as the values of the specification table are at the MPPT. The manufacturer assures an efficiency between 15% to 20% and the value obtained with the Matlab script developed is 19% and so it can be said that the values assumed for voltage and current are correct. Also, the maximum power is computed by the script and it gives a value of 0.73 W which is very close to the one that is specified.

5.2. Assembly and performance

As it has been said in the previous section, buying individual solar cells allows the assembling in any way needed and wanted and therefore it has been concluded that the optimum device is going to be shaped as an array of four individual solar cells connected in series. In the schematic below (Fig. 5.2), the disposition of the solar cells is shown. As indicated, the red line represents the positive sign and the black line, the negative sign, specifying the direction of the current flux.

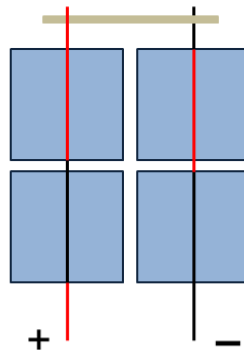


Fig. 5.2. Schematic of the array of solar cells

In addition, on an individual solar cell the current flows from bottom to top. The series connections must be done by welding tabbing wire, which is included in the pack of solar

cells that has been ordered along with a bus wire and a flux pen, to the solar cells. They are connected to one another with a long portion of tabbing wire that goes from the back of one solar cell to the upper part of the other.

So as to make the square-like shape, the second and the third solar cells have been joined with a bus wire, which is a slightly wider than the tabbing wire. The tabbing wire is easily welded to the cells, by just applying the flux pen softly on the path of the solar cell that needs to be attached the wire to, then joining the wire and the cell together and applying heat with a soldering iron, applying some pressure. The flux prepares the materials that have to be joined and lets the soldering iron to move fluently.



Fig. 5.3. Upper and lower sides of a solar cell with tabbing wire

In the other hand, the welding of the tabbing wire with the bus wire requires the use of tin to link them together.



Fig. 5.4. Bus and tabbing wire welding

The welding process must be done very carefully as the solar cells are extremely fragile. In order not to break any of the cells small bands of tape have been used, as it can be removed easily when the welding process is over. Once the welding is done both the current and voltage of the circuit have to be tested with a multimeter.

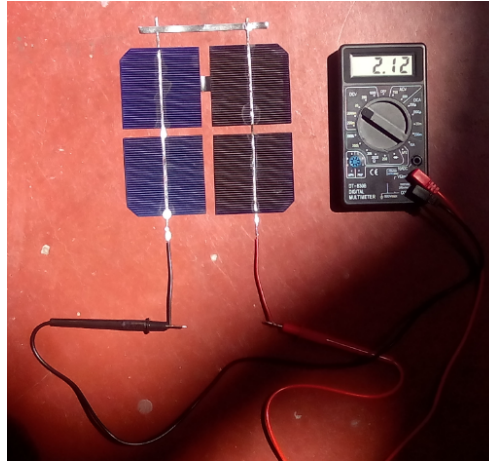


Fig. 5.5. Voltage performance test

When the solar cells are welded, the programming part of the project starts. For this part, a combination of the softwares of Matlab and Arduino are used.

5.3. Implementing Arduino

It is true that by just using a multimeter, the values of voltage and current can be taken at any moment. However, this is not a good method when these values have to be measured on the high altitude balloon. The solution for this problem is the use of Arduino. So as to test the performance of the Arduino equipment, the experiments of this bachelor thesis are done with these software and hardware.

Arduino is an open-source software and hardware, very accessible and easy to implement. With the simplest board, the Arduino UNO, voltage and, using the ACS712 sensor for the current can both be measured. For the collecting of the data, the "Matlab Support Package for Arduino Hardware" is used [34]. This package allows reading, writing and analyzing data from Arduino sensors and store the values in Matlab variables. As soon as package is installed, the Arduino board can be controlled with Matlab with the following script:

```

1 install_arduino
2
3 a=arduino('COM3');
4
5 n=1;
6 numData=10;
7 timeData=1; %time in seconds; frequency of sampling
8 sensitivity=0.185;
9
10 while n<=numData
11
12     vectorVoltage(n,1)=a.analogRead(0)*5/1023;%voltage in A0
13     sensorcurrent=a.analogRead(1)*5.0/1023; %current in A1
14     current=(sensorcurrent-2.4976)/sensitivity;

```

```

15     vectorCurrent(n,1)=current;
16
17     pause(timeData);
18
19     n=n+1;
20
21 end

```

The first line of the script installs the Matlab package that will allow the connection between Matlab itself and the Arduino. The script that defines the package must be in the same path as the one that is being used, as well as the rest of the files of the package. Then, the "a" variable is associated to the Arduino port used, which in this case is the COM3.

Once an experiment is done and the data stored, another script in Matlab with an structure has been created, in order to organize all the results and then plot the different curves with ease. As it can be seen in Figure 5.6, the scheme of the structure, called "Experiments" is divided in sections corresponding to the number of the experiment that is being performed. Inside each experiment, there is an array for each load, and for each load there exist both current and voltage data. The current and voltage are divided in data and average, as three samples are going to be taken for each load and then the average value will be used for a more exact calculation of the curve.

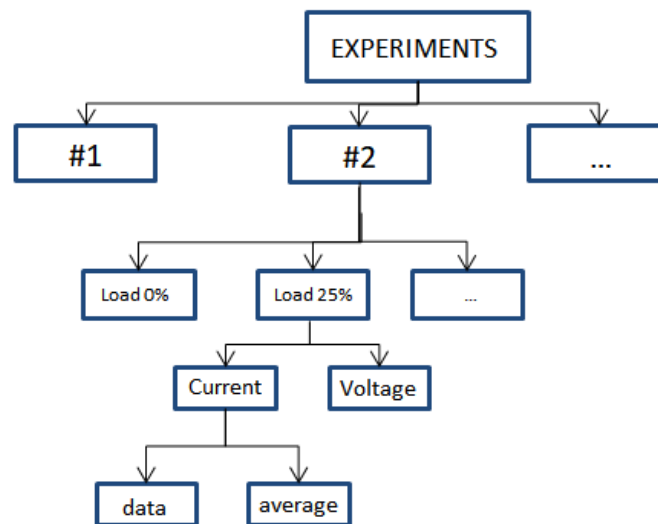


Fig. 5.6. Scheme of the structure in Matlab

5.3.1. Voltage measurement

In Arduino, voltage values can be measured without using an additional sensor, as the Arduino UNO can test the voltage itself. The analog read function of Arduino measures the voltage with an scale from 0 to 1024 bits, which are converted to volts by using a

conversion factor, as voltage goes from 0V to 5V. The board has several analog ports and for the voltage measuring we are going to use the A0. Firstly, the positive wire of the solar cells needs to be connected to the analog pin A0 and the negative wire to the GND port (ground), as seen in Figure 5.7.

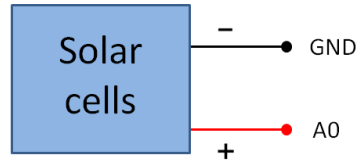


Fig. 5.7. Voltage connections in Arduino UNO

Then, the Arduino code implemented in Matlab (Section 5.3) is run. A *while* loop is executed until the number of samples that need to be taken is reached, which is defined with the variable "numData". The voltage values are stored in a vector called "vectorVoltage".

5.3.2. Current measurement

In order to be able to measure the current, an additional sensor connected to the Arduino UNO is needed. As it has been said previously, the sensor selected is the ACS712. This specific sensor uses the Hall effect, which it is produced when a magnetic field is applied perpendicular to a current conductor material the electrons are pushed to the edges and a voltage appears.

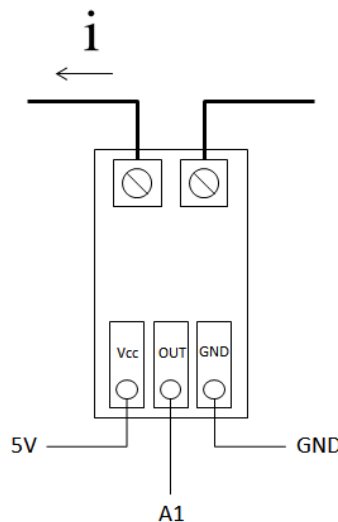


Fig. 5.8. Current sensor connections in Arduino UNO

Then, this voltage can be converted into current in the Matlab script (Section 5.3) taking into account that the sensitivity is 185 mV and again using a conversion factor to get

the voltage value from the measured bits that are later converted into current with the expression 5.1. The values of the current are stored in a vector called "vectorCurrent".

$$current = (sensorcurrent - 2.4976)/sensitivity \quad (5.1)$$

The connections of this sensor are described in the scheme of Figure 5.8. The V_{cc} port is connected to the 5V output of the Arduino board; then the OUT goes to the A1 pin of the board (we have chosen A1 pin as the pin A0 is being used to measure the voltage; finally, the GND to the ground pin of the Arduino UNO. The sensor measures the current by inserting into the two upper holes the wire where the current flows, doing it as a series connection.

5.3.3. Load variations

Lastly, in order to get the values of current and voltages with different loads, we have implemented a potentiometer of 100 Ω . By changing the resistor value we will get distinct values of voltage and current that will be plotted together lately to draw the characteristic I-V curve for each experiment conditions.

In this case, the potentiometer has three pins. The first one is connected to the ground or the negative wire of the solar cells, the one in the middle goes to the positive wire of the solar cells and the left one is not connected, so the potentiometer can be used as a variable resistance.

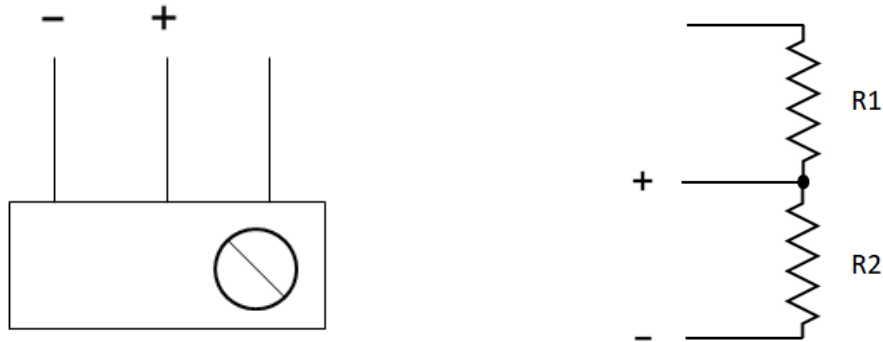


Fig. 5.9. Potentiometer schemes

On the left hand side of Figure 5.9, the scheme of the potentiometer with its connections is represented. The scheme on the right side of the same figure presents the internal schematic of the so called potentiometer. By connecting just two out of the three pins the load is changed as by spinning the wiper pin to the left the value of the resistor R2 increases and the opposite thing occurs when spinning the wiper to the right, R2 decreases and R1 increases; being the total resistance of the potentiometer the addition of R1 and R2.

5.3.4. Final circuit

However, for the experimental design, the measurements need to be done at the same time, in order to get the pairs of values well. In the schematic of Figure 5.10, the final configuration of the circuit, with both sensors and the potentiometer integrated, is shown.

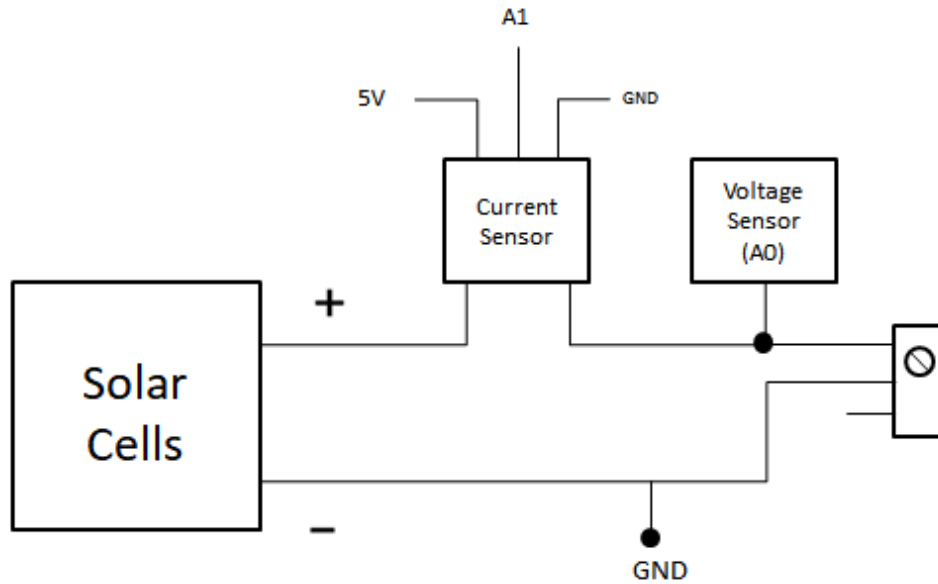


Fig. 5.10. Final circuit connections scheme

5.3.5. Arduino in the high altitude balloon

As the computer can not be placed in the box attached to the high altitude balloon, a different way to feed the Arduino UNO board is needed. The board must be fed with a voltage higher than 6 V, if it is lower the Arduino would not work properly, and less than 9 V, a higher voltage would produce serious damage of the board. There are two possible solutions for this problem. The first solution is to use an Arduino connector and attach a battery of 9 V [35]. Batteries are reliable and cheap but, the problem with batteries is that they do not last a lot of time.

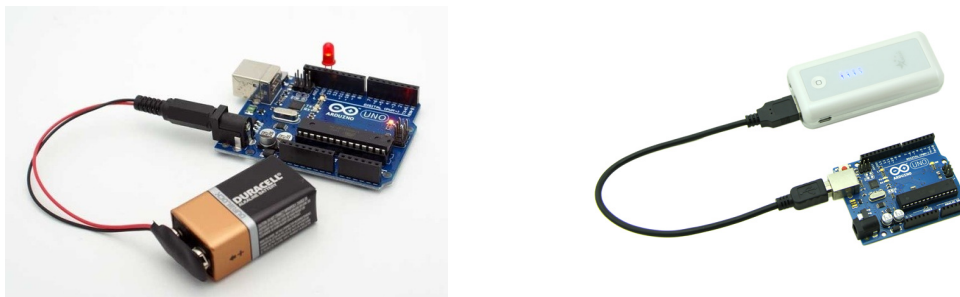


Fig. 5.11. Types of Arduino UNO feeding solutions

The second solution would be the use of a USB powerbank. There is no needed to buy an additional connector due to the USB port that is included on the Arduino board that was used for the connection with the computer and they can be recharged so the powerbanks can be used many times [35].

Furthermore, as the Arduino is not connected to the computer and it does not have internal storage, an external chip that can read microSD cards to save the data is required. An extra part of code would be needed. An external microSD reader has been chosen over the SD reader chip because it is slightly cheaper, however the operational differences between using a SD card or a microSD card are non existent. The connections with the Arduino UNO board can be seen in Figure 5.12

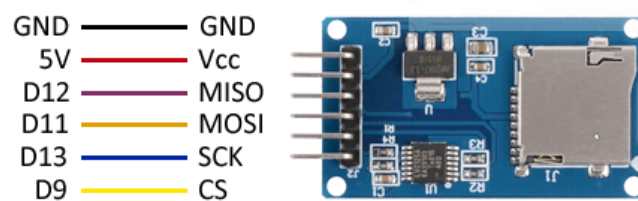


Fig. 5.12. Arduino UNO to microSD reader connections [36]

6. THEORETICAL MODEL

Before doing the experiments to see the variations of the parameters of the solar cells, a simulation in Matlab has been designed. By implementing the correlations of the voltage and current of a solar cell, the I-V curve, the power at every moment of the curve and the maximum efficiency point can be obtained. This results will be compared with the experimental data obtained (Chapter 7).

6.1. Matlab simulation to predict the I-V curve

In Annex I (A), the Matlab script used for the obtaining of the I-V curve can be found. Before running the script, the values of the open circuit voltage (V_{oc}), short circuit current (I_{sc}), area of the solar cell, global radiation and ambient temperature need to be filled in.

Then, in the script, all the formulas (quote formulas del apartado de las PV cells) that relate voltage and current with the parameters they depend on are written. By giving values from 0 to the quantity of the V_{oc} to the voltage, a current value for each voltage is computed. Finally, with the plot function the I-V curve is shown on the screen (Fig. 5.1). Furthermore, a prediction of the I-V curve of the four solar cells array that will be launched with the high altitude balloon can be shown in Figure 6.1 with the blue line.

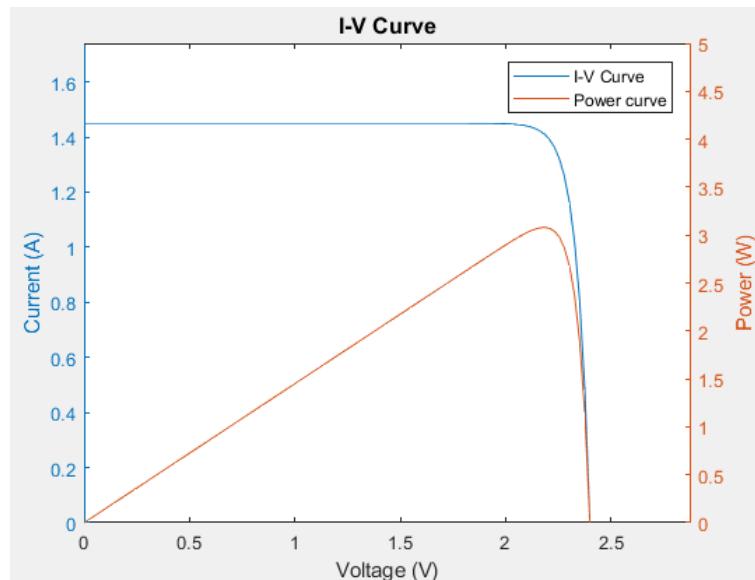


Fig. 6.1. Theoretical I-V curve for an array of four solar cells

6.2. Power curve

In the case of the power, the curve is obtained by multiplying the vectors with the pairs of values for voltage and current. In order to see on the same plot as the I-V curve the representation of the power, the command *yyaxis right* is used, so that the scale of the power curve is adjusted to the I-V curve. The prediction of this theoretical curve is represented in Figure 6.1 with the red line. Consequently, the power is four times the power of just one solar cell.

Moreover, the maximum power point is calculated and then the efficiency is obtained with the formula (4.8) of Section 4.3.

6.3. I-V curve shifts

Some shifts on the curve are expected when the temperature and the radiation of the cell change. However, as the voltage and current values also depend on these parameters, the approximation can only be made by knowing beforehand the open circuit voltage and the short circuit current.

7. EXPERIMENTAL SETUP

In this chapter, several experiments have been carried out in order to find the characteristic I-V curve of the selected solar cells, as well as the power and efficiency. Also, the changes of the open circuit voltage and the short circuit current with radiation and cell temperature variations. The final installation done to perform the experiments is shown in Figure 7.1.

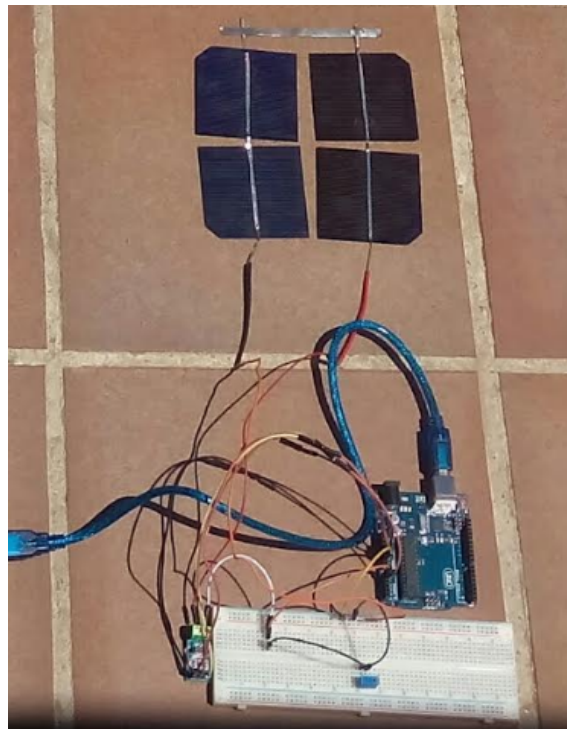


Fig. 7.1. Final installation

7.1. Characteristic I-V curve

The first experiment has the purpose of characterizing the I-V curve of the solar cells array at standard conditions. The cells are placed facing the Sun with an incidence angle of 0° . After preparing the circuit with the sensors to measure the voltage and current following the schematic of Figure 5.10, the code for working on Matlab (Annex I) has to be compiled and uploded to the Arduino UNO board. Then, the Matlab script for working with the Arduino needs to be run on the Matlab software. After doing all this setup, everything is prepared for collecting the data.

The program will take three values of voltage and three values of current, to make sure that all the values are okay and the sensors are not failing. The data is collected every second. The time interval can be changed on the Matlab script anytime required. Firstly, the value of the open circuit voltage will be obtained by removing the potentiometer from

the circuit. Next, the potentiometer will be placed at its maximum load and the data collected. This last process will be repeated several times by gradually decreasing the load.

Later, all the data will be saved in the Matlab structure (Section 5.3) so it will be easier to plot the curves.

7.2. Incidence angle variation

Once the I-V curve at standard conditions is obtained, the study of the cell efficiency at different radiation intensities can be performed. To do that the incidence angle of radiation is changed and the process for collecting the data will be done. The incidence angle is changed by varying the slope of the solar cells. The slopes at which current and voltage will be measured are: 0° (parallel to the ground), 30° , 45° , 60° , 75° and 90° (perpendicular to the ground). This experiment will allow to determine the variations that the performance of these solar cells undergo.

7.3. Temperature variation

The third and final test will be done by changing the temperature of the solar cells. A temperature sensor will be placed on the cell and temperature will be changed with the effect of ice and hot bags. The purpose of this experiment is to study the changes in open circuit voltage and short circuit when temperature changes in these particular solar cells.

8. RESULTS

8.1. Characteristic I-V curve

As it has been explained in Section 7.1, with this experiment the I-V curve of the array of solar cells is defined. The experimental curve (red line) is compared with the theoretical results (blue line) obtained using the Matlab script of Chapter 6. The value of the solar radiation² has been taken from Aemet Database (quote). The ambient temperature is the one measured with the sensor the day of the experiment³. It is shown that the shape of the experimental curve is similar to the theoretical one and that the curve can be smoothed by taking more measurements.

Furthermore, the gap in the zone where the point of maximum efficiency is achieved is produced due to several factors that affect the cells and are not taken into account in the theoretical model, such as the sensibility of the tools used to measure voltage and current or the error in the measurements. Also, the scattered radiation due to the clouds that were present the day of the experiment or the pollution accumulated in the troposphere.

The deviation between the ideal and the experimental curves is also affected by the imperfections that may have been created on the cells surface during their manipulation while assembling them together or due to the transportation from the workspace to the place where the measurements are carried out.

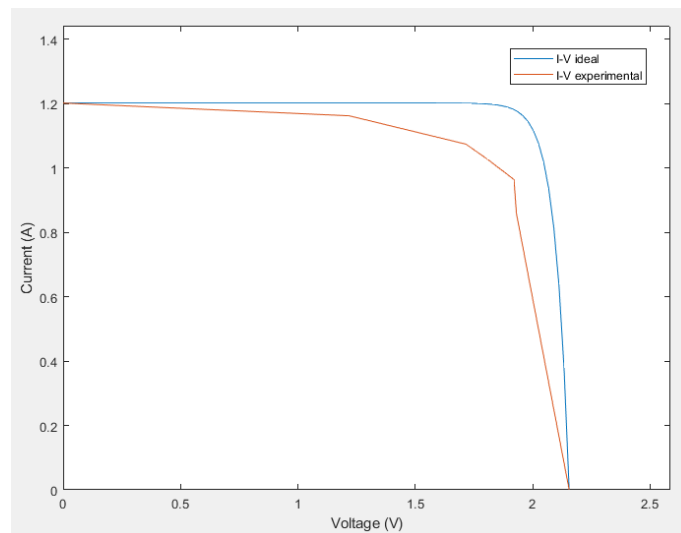


Fig. 8.1. I-V curve comparison

Additionally, the sensitivity of the current sensor has limited the measures, as current

²The radiation was 723 W/m²

³The temperature was 24.3°C

values lower than 0.185 V could not be considered. Despite all these factors, the experimental curve can be considered a good characterization of the correlation between the current and voltage of the array of solar cells.

Next, the experimental curve of the power (blue line) is obtained by using the data from the previous experiment and it is compared with the ideal one (red line) at the same conditions that were described before. Due to the factors explained before, these curves do not fit, although the shapes are pretty similar. It is shown that the voltage where the power is maximum on the ideal curve corresponds to the voltage where the power is at its maximum on the experimental curve. What truly changes the power value is the current as the radiation incident on the cell is lower than the radiation coming from the Sun due to imperfections and dirtiness of the present solar cells.

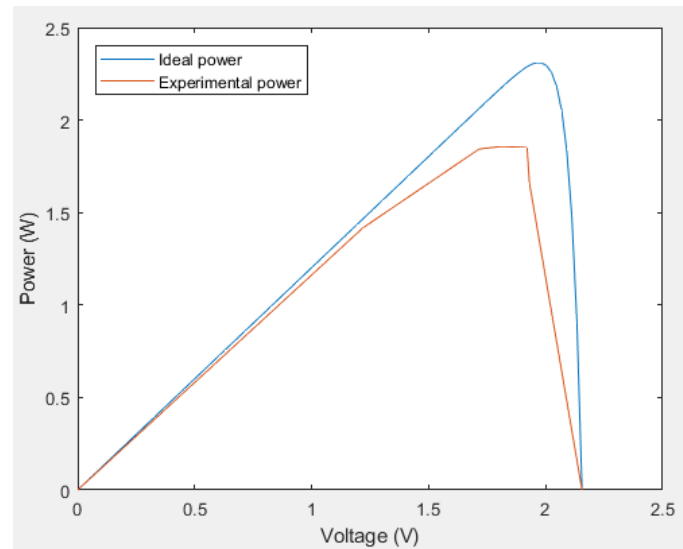


Fig. 8.2. Power curve comparison

Additionally, by using the plot of Figure 8.2, the maximum power on the experimental curve value can be seen, that is 1.86 W, which is almost 1 W of difference with respect to the value at the same place of the theoretical model, lowering the efficiency from almost 19% to slightly above 15%.

8.2. Incidence angle variation

For this part, the angle of incidence is changed by varying the position of the solar cells with respect to the horizontal surface. With this variations the radiation incident on the surface is different at every position and the changes in the V_{oc} and I_{sc} with solar radiation are determined.

In the left part of Figure 8.3, it is shown that the open circuit voltage does not change significantly when the radiation incident on the cells is altered, as it was theoretically

expected (quote). Nevertheless, it is expected that the decrease in radiation affects directly the short circuit current by dropping it. In the right part of Figure 8.3, the plot of the short circuit current versus the slope angle is represented and it is shown how it decreases when the radiation hitting the surface of the cells is reduced. At first, when the slope angle μ is placed so the incidence angle θ is 0° , the I_{sc} is at its maximum and then the declination starts when this angle is higher.

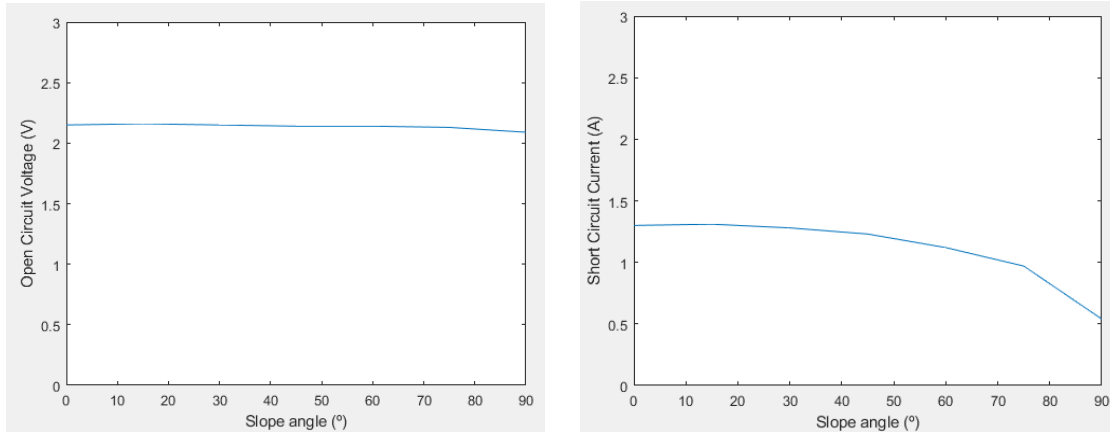


Fig. 8.3. V_{oc} and I_{sc} changes with slope angle

8.3. Temperature variation

In this last experiment, in contrast with the previous one, the short circuit current is expected to remain almost constant when temperature changes. However, in this case, voltage is expected to decrease with an increment in the cell temperature, as it depends on it (Section 4.3).

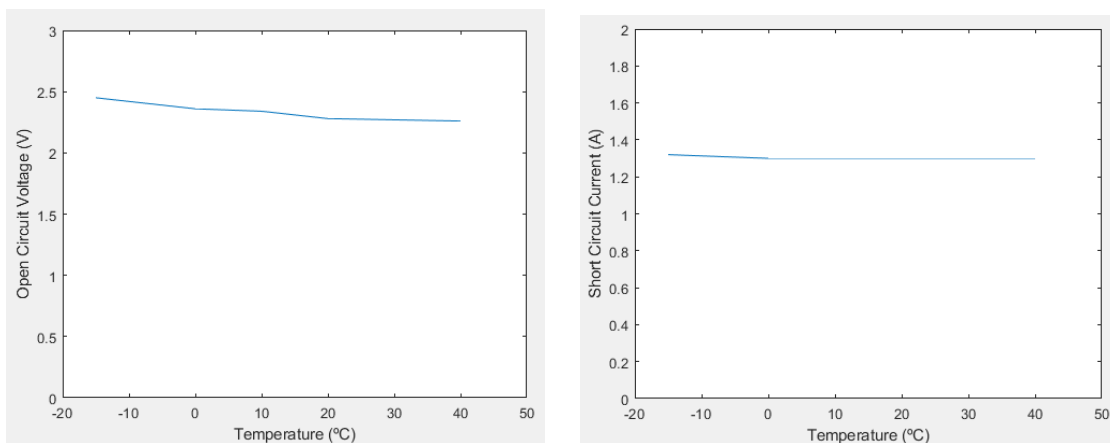


Fig. 8.4. V_{oc} and I_{sc} changes with cell temperature

As the right hand side plot of Figure 8.4 shows, the short circuit current slightly changes with temperature. Nevertheless, the graph on the left hand side proves that the open circuit voltage indeed changes with temperature, being higher when the temperature is lower [24].

It can also be noted that the I_{sc} of the experiments related with temperature and incidence angle changes is slightly higher than the value obtained for the same parameter in the first experiment of I-V curve characterization. That is because the experiments were carried out in different days and the Sun radiation on the day of the first experiment was lower than the radiation value measured on the days when the rest of the experiments were done⁴.

8.4. Load variation

Lastly, both voltage and current have been plotted versus the load applied on the circuit by using the data obtained in the first experiment (Section 8.1).

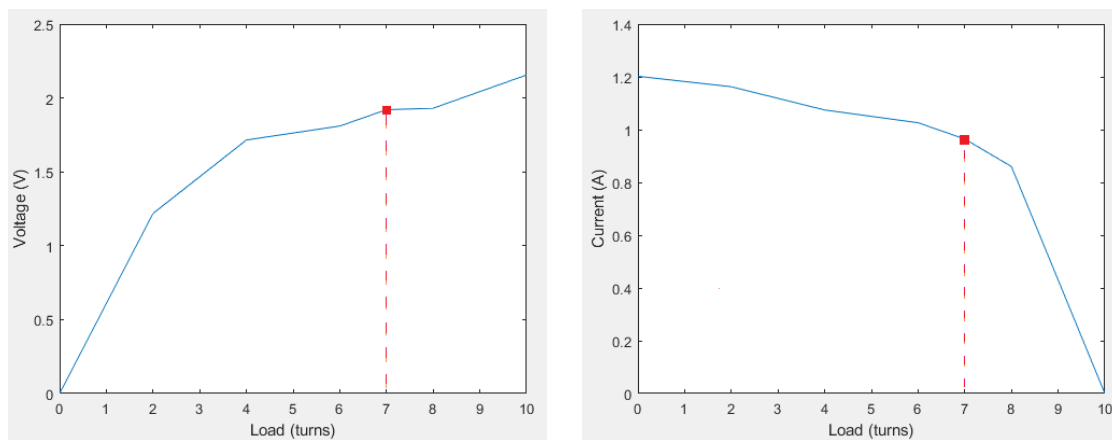


Fig. 8.5. V_{oc} and I_{sc} changes with load variations

In Figure 8.5, it is shown how the voltage increases when the load gets higher until reaching the open circuit voltage at the maximum load. In the other hand, the current decreases with load, starting at the I_{sc} when the load is null and reaching a zero value when the load is maximum and the circuit is opened.

By analyzing Figure 8.2, it can be seen that the point of maximum power, at 1.86 W, is obtained when the voltage has a value of 1.93 V. Then, looking for that voltage value in Figure 8.1, the current value is obtained as well, with a value of 0.96 A. From graphs of Figure 8.5, it is shown that the potentiometer at the maximum power was given 7 turns, which corresponds to an approximate value of 70 Ω .

⁴The radiation value of the day the temperature and angle variation experiments were done was 876 W/m²

9. THERMAL INSULATION OF THE DEVICE

After deciding which solar cells are going to be sent to the stratosphere on the high altitude balloon, the need of a good insulation appears. As seen in Chapters 7 and 8, cell temperature variations affect the efficiency of the cell. In order to operate with the highest possible efficiency the highest amount of time, an optimum insulation of the PV cells will be key for the correct functioning of the high altitude balloon experiment.

9.1. Parameters that affect the temperature of a solar cell

Deciding which insulator is going to perform better with the selected cells, depends on how the parameters that change the cell temperature vary (within the altitude range that the high altitude balloon is going to cover); that is because the temperature is the basis of obtaining a good performance of the pn-junction of the semiconductors that define the solar cell. These parameters are the ambient temperature, the wind and the solar radiation.

Firstly, the ambient temperature is considered. In Figure 3.1, temperature is represented against altitude. The estimations place the high altitude balloon bursting approximately at 28,000 meters high so that the temperatures that the cell need to withstand go from -50°C to $+20^{\circ}\text{C}$. In the troposphere, the temperature starts at $+20^{\circ}\text{C}$ and decreases with altitude until -50°C at 10 kilometers high. Then, there is the tropopause, where the temperature remains the same at -50°C . Finally, in the stratosphere portion the balloon is going to cover, the temperature increases slowly until reaching around -40°C at 30 kilometers high.

Then, the following factor considered that changes the cell temperature is the wind. Its speed and temperature can cool down or heat up the solar cells through forced convection, as the convection coefficient depends on the velocity of the wind. The convection coefficient affects the heat dissipated by convection as shown in Equation 9.1, being A_c the area of the cells exposed to the wind, T_c the temperature of the cell and T_a the ambient temperature.

$$Q = hA_c \cdot (T_c - T_a) \quad (9.1)$$

Moreover, the convection coefficient is calculated from the Nusselt number following Equation 9.2. It also depends on the thermal conductivity of the air (k) and the characteristic length (L). The Nusselt number can be calculated by using Reynolds and Prandtl numbers.

$$Nu = \frac{hL}{k} = ctn \cdot Re^m \cdot Pr^n \quad (9.2)$$

Then, the Reynolds number is calculated with Equation 9.3, which depends on air density (ρ), its velocity (v_{wind}) and viscosity (μ) along with the characteristic length (L).

$$Re = \frac{\rho \cdot v_{\text{wind}} \cdot L}{\mu} \quad (9.3)$$

And finally, the Prandtl number is obtained with Equation 9.4. It depends on the specific heat (c_p), the viscosity (μ) and the thermal conductivity (k) of the air.

$$Pr = \frac{c_p \cdot \mu}{k} \quad (9.4)$$

Moreover, the wind is produced when the temperature or pressure of the air changes. In the troposphere, the changes in wind speed are defined by the thermal and the geostrophic wind [37]. First of all, the geostrophic wind is the resultant force coming from the balance of the pressure gradient and the Coriolis force. In the Northern Hemisphere, it goes from high to lower pressures and depends on the rotation velocity of the Earth and the latitude.

In the other hand, the thermal wind, which is a theoretical concept created to calculate the variations of wind with altitude, changes with temperature, and in the Northern Hemisphere goes from colder to warmer regions. In the tropopause, there is no vertical air streams and the horizontal wind can be neglected. However, in the stratosphere there exists horizontal air currents that can reach high speed ranges, from East to West in the upper Hemisphere. In order to take into account these wind gusts, a wind predictor software can be used, like *Ventusky* [38]. *Ventusky* is a real time weather mapping tool with high forecasting accuracy. One of the tabs allows the user to know the wind speed up to 30 kilometers high.

Finally, the Sun radiation also affects the temperature of the cell, increasing it when radiation rises. The temperature of the solar cells (T_c) can be approximated with the formula 9.5 which relates it with ambient temperature (T_a) and solar radiation (G), by knowing the nominal operation temperature (T_{NOCT}) of the cell [39].

$$T_c = T_a + \frac{T_{\text{NOCT}} - 20}{800} \cdot G \quad (9.5)$$

This formula is used on the Matlab script of Annex I in order to predict the I-V curve by knowing radiation and ambient temperature values.

9.2. Insulation model

The most common encapsulation structure for insulating the solar cells is by using ethylene-vinyl acetate (EVA). The disposition of the materials follows the scheme of Figure 9.1.

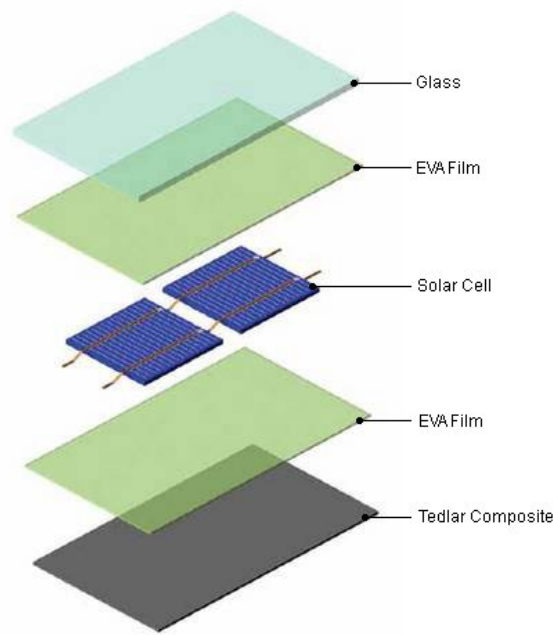


Fig. 9.1. Solar cells insulation array

Solar cells are covered in both sides with EVA. Its is a thermoplastic constituted by ethylene and vinyl acetate. The average melting point is 100°C and changes depending on the vinyl acetate percentage on the compound. Additionally, EVA has great resistance to cracks and therefore it also protects the cells that are inside the encapsulation from breaking, and more importantly, it has a wide range of temperature resistance. Thus, the durability of this material is very high. It also allows to easily glue the cells to other protective layers and it is almost transparent, allowing great transmission of the Sun radiation. Another advantage of EVA is that it avoids humidity and dust reaching the solar cells [40].

In order to increase the temperature range in the colder region and protect the solar cells from dirt and humidity, a polyvinyl fluoride (PVF) layer is attached to the lower part of the EVA encapsulation, as a backsheet. The polyvinyl fluoride is commonly known as Tedlar, which is the name the US company DuPont uses to define the so called material. The PVF is a thermoplastic fluoropolymer, manufactured as a thin layer or film and used as coating for protection. This plastic bears temperatures within -70°C to $+110^{\circ}\text{C}$. As the lower temperatures that the cells need to withstand are around -50°C , this material suits perfectly the requirements of the high altitude balloon experiment. It has also low permeability, so moisture will not penetrate through the cells and high strength, thus it will increase the protection of the solar cells against collisions [41]. However, Tedlar is usually combined with other polymers so the price is not too high. The Tedlar composites are made with EVA and other polymers such as PET (polyethylene teraphthalate).

The Tedlar layer is not transparent and therefore, it cannot be placed in the upper part of the encapsulation structure as radiation needs to reach the silicon cells. In this case, a glass is used. The glass needs to have high transmittance and low reflectance values. The

best glass to fulfill these requirements is a low iron rolled glass. According to the technical specifications of AEON glass company (one of the most important manufacturers of quality glasses in the world), the low iron rolled glass has a visible light transmittance of 91%, a reflectance value of 7% and UV transmittance of 87%. Also the regular thickness of these glasses is around 3 mm.

Insulation		
Material	Thickness (mm)	Thermal Conductivity (W/mK)
Glass	3	0.9
EVA (both layers)	0.5	0.35
Tedlar	0.1	0.2

Table 9.1. Insulation materials

Additionally, a further insulation level can be reached by the implementation of a transparent insulation material (TIM) [42], which are made of thin films of plastic or glass and have a honeycomb structure that stops the air from passing through its pores and they are transparent, allowing radiation to pass through the material and to the solar cells. Nevertheless, this option is not good for small solar panels as it is sold in large amounts (these prices are acceptable only for the big industry). However, another solution for the improvement of insulation can be easily done by making vacuum gaps between the EVA and both the glass and the Tedlar layers.

The implementation of the structure is done with the following steps. First of all, the cells must be cleaned deeply before starting the assembling of the insulators. Then, the solar cells are covered by the EVA layers. EVA is very ductile at high temperatures and, with the use of a hot gun, it can be heated so that the material adapts and fits better, covering the cells completely.

Afterwards, the cells are mounted on a frame, that is done with wood and covered with an epoxy resin so it becomes insulated and sealed, and the Tedlar layer is implemented below the solar cells. A vacuum gap between the EVA and the Tedlar can be created with a vacuum cleaner. Finally, the same vacuum gap can be obtained between the cells and the low iron rolled glass, which is placed covering the upper part of the solar cells.

9.3. Manufacturers selection

Lastly, the selection of the manufacturers have been done studying the relation between price and quality and the optimum specifications for each insulation layer. The thickness of the layers follows the model proposed by a research article of the University of Arkansas (USA), which follows the general specifications used in commercial solar panels [39]. The manufacturers that have been selected for each insulation layer are:

- The EVA will be purchased from the manufacturer Vikocell.
- The Tedlar will be bought from Vikocell as well. The Tedlar selection is a composite of Tedlar with PET and EVA. It is thicker than the specifications requirements, 0.3 mm, but the price is much cheaper than purchasing a solo Tedlar film. The problem with only needing a small amount of insulation materials is that they are sold in big quantities. The materials proposed for the experiment are the ones with the lowest possible amount so the spare materials are as reasonable as possible.
- The low iron rolled glass will be bought from the manufacturer AEON Glass.

Material	Manufacturer
EVA	Vikocell
Tedlar composite	Vikocell
Glass	AEON Glass

Table 9.2. Insulators manufacturers

10. RADIATION FILTERS

Commercial models of photovoltaic solar panels are not equipped with radiation filters as the atmosphere itself acts as a natural filter for radiation due to the absorption of several wavelengths at different altitudes. However, as the high altitude balloon that will carry the solar cells will go through the troposphere and to the stratosphere, radiation may increase with the altitude, as the concentration of the absorbers changes. This leads to a research on the optical properties of the atmosphere and their variation with altitude and whether filtering the incident radiation will be needed.

As explained in Chapter 3, the atmosphere is constituted by gases, liquids and small particles. These components define the optical properties of the atmosphere, that include absorption, scattering and emission.

Above all, the absorption [15], which is directly related with the atmospheric transmittance (fraction of incident radiation passing through a sample and thus through the atmosphere), will be considered. The main atmospheric absorbers are water vapor (H_2O), carbon dioxide (CO_2), oxygen (O_2) and atomic oxygen (O) and ozone (O_3). Firstly, the water vapor absorbs radiation from 0.7 to $8\text{ }\mu\text{m}$, accepting almost 100% of $6\text{ }\mu\text{m}$. Then, the CO_2 acts as a temperature regulator of the Earth and absorbs radiation from infrared wavelengths from 2.5 to $4.5\text{ }\mu\text{m}$ and from 15 to $25\text{ }\mu\text{m}$. Next, the oxygen, that takes over wavelengths below $0.1\text{ }\mu\text{m}$. Finally, the Ozone, which absorbs radiation from 0.1 to $0.3\text{ }\mu\text{m}$ and in the microwaves region.

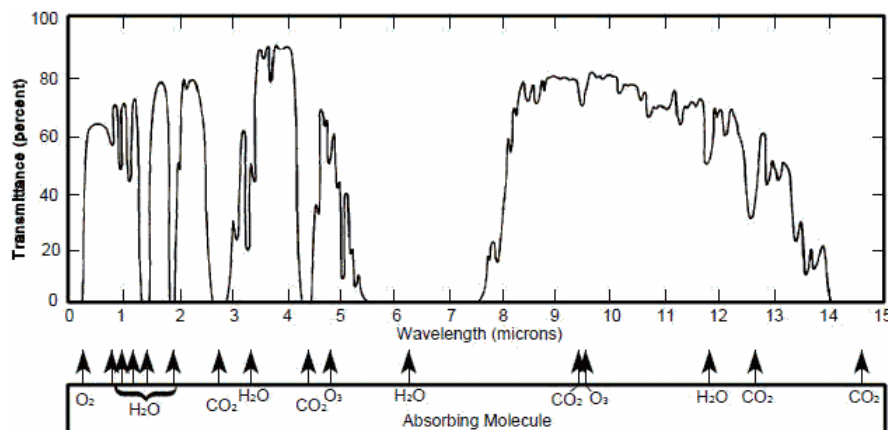


Fig. 10.1. Absorbers in the atmosphere [43]

Knowing the distribution of these absorbers through the atmosphere is mandatory to determine if the use of a filter for some radiation wavelengths will be necessary. In figure 10.2, the red line indicates the maximum altitude that can be reached by the high altitude balloon. It is shown that the mixing ratios of the different components are constant until

an altitude of 10 km, that is when the troposphere ends. However, the water vapor concentration decreases from the surface of the Earth until the tropopause, where it remains constant and from there to the upper layers it maintains its concentration. The most significance variation of an absorber is the Ozone's, as from 20 km, the mixing ratio starts to grow exponentially, that is where the Ozone layer is located.

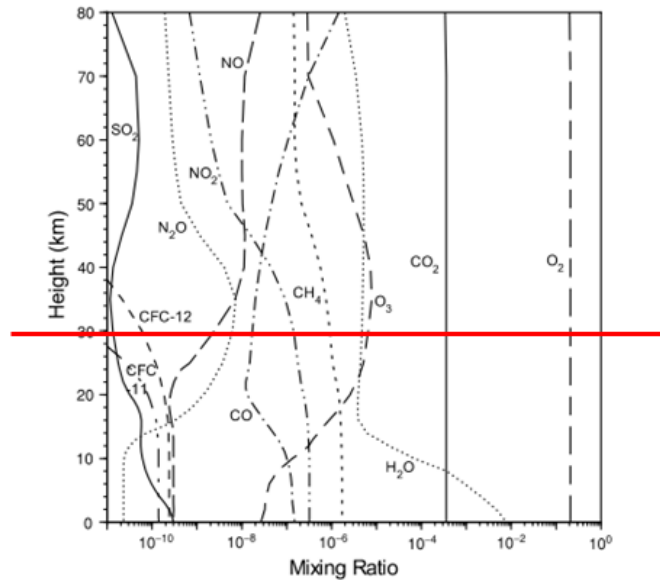


Fig. 10.2. Mixing ratio of absorbers with altitude [15]

Moreover, in Figure 10.3, the reduction of the direct irradiance is represented. It can be seen that the direct radiation that hits the surface of the Earth is reduced up to 400 W/m^2 and the factors that affect the most this reduction are the water vapor and aerosols.

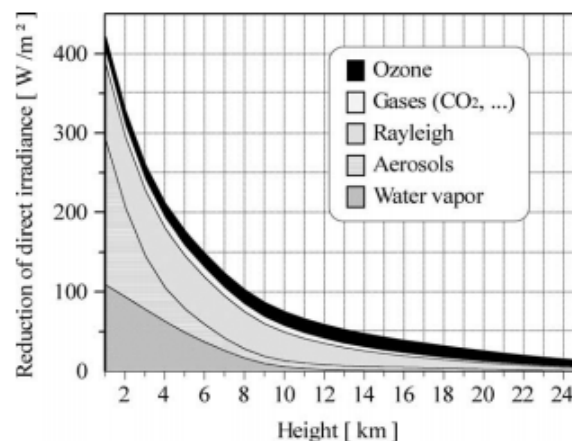


Fig. 10.3. Reduction of direct radiation [44]

Furthermore, several researches have studied the changes in the output power depending on the color of the light incident on a solar cell. By using colored polythene filters to change the wavelength of the light reaching the photovoltaic cell, they have concluded

that the color of light indeed affects the output power and therefore the efficiency of solar cells [45]. According to an article of the National Institute of Technology Maulana Azad (India) [46], it is shown that the highest efficiency is achieved without a filter, as the solar cells can receive all the photons. However, this efficiency is closely followed up by the one get with a red filter.

In solar cells, the Sun radiation in between the wavelength range of $0.4 \mu\text{m}$ to $1.1 \mu\text{m}$ has enough energy to push the electrons of the pn-junction out of their bonds. Table 10.1 [47] shows the wavelengths of the visible light, ultra violet (UV) and infrared (IR) radiations. It can be seen that the UV radiation has a very little contribution in the sunlight that reaches the surface of the Earth and that most of the electricity generated by solar cells come from the visible light, as the spectrum happens to meet their optimum wavelength range. The radiation that is not absorbed by the cells is converted into heat that affects the efficiency, decreasing it.

	Wavelength	Percentage of Sunlight
UV	0.01-0.38 μm	7%
Violet	0.38-0.45 μm	46%
Blue	0.45-0.495 μm	
Green	0.495-0.57 μm	
Yellow	0.57-0.59 μm	
Orange	0.59-0.62 μm	
Red	0.62-0.75 μm	47%
IR	0.75-1000 μm	

Table 10.1. Wavelengths of Sun radiation

As a conclusion, and considering all the previous factors, the use of a protection filter for the solar cells is considered unnecessary as the only part of the solar radiation that is going to change significantly with respect to the troposphere below 30 km of altitude is the ultraviolet. But, as the balloon will roughly reach the ozone layer and the time it will spend there will be very short.

Additionally, something else that needs to be taken into consideration is the higher value of the radiation that is reflected by the Silicon, more than 35%. An anti reflective coating [48], or ARC, can be used in order to improve the efficiency of the solar cells. The coating can be applied either on the solar cells or on the glass cover and they are made out of silicon dioxide (SiO_2), titanium dioxide (TiO_2) and silicon or boron nitrides. Fortunately, it is already applied to most of the glasses used for the protection of solar cells and it is included on the glass that was proposed on Chapter 9.

11. COSTS ANALYSIS

In this chapter the cost analysis of the project is explained in detail. The duration of the project that has been taken into account is 360 hours. In Table 11.1 the material costs are displayed. The third column, that corresponds to the "Price per unit" refers to the cost of the units used in the column of "Quantity".

Material	Quantity	Price per unit (€/u)	Cost (€)
Solar cells	4 units	0.55	2.20
Tab wire	0.50 m	0.51	0.25
Bus wire	0.15 m	0.74	0.11
Flux Pen	1 unit	3.39	3.39
Tin	3 g	0.07	0.2
Wires	0.2 m	0.06	0.01
Connectors	10 units	0.06	0.59
Arduino	1 unit	6.29	6.29
ACS712 sensor	1 unit	5.00	5
Temperature sensor	1 unit	11.76	0.43
EVA	0,0365 m ²	7.11	0.13
Tedlar composite	0,0182 m ²	1.70	0.01
Glass	0,0182 m ²		
Total			18.61

Table 11.1. Material costs

Then, Table 11.2 refers to the costs of the tools needed for the accomplishment of the project. The amortization of each tool is shown; the computer and Arduino UNO amortization are calculated assuming 120 days of work and a useful life of 3 years, next the welder is calculated assuming 4 days of use and 10 years of useful life.

Tool	Quantity	Price per unit (€/u)	Cost (€)
Computer	1 unit	599.99	65.64
Arduino UNO	1 unit	20.00	2.19
Welder	1 unit	10.99	0.02
Total			67.86

Table 11.2. Tool costs and amortization

Finally, the costs due to human resources. The salary of both the Junior Engineer have been assumed taking into account the hours of work, the difficulty of the work and the education level.

Human Resource	Salary (euro/h)	Working hours (h)	Cost (euro)
Junior Engineer	10	360	3600
Tutor	100	15	1500
Total			5100

Table 11.3. Human resource costs

In Table 11.4, a summary of all the previous costs along with the total cost of the project is shown.

Concept	Cost (€)
Materials	18.61
Tools	67.86
Human resources	5100
Total	5186.47

Table 11.4. Total costs

12. CONCLUSIONS

First of all, the purpose of this bachelor thesis was to develop an experimental design to obtain voltage and current values of a set of solar cells that are attached to a high altitude balloon, in order to study their performance and behavior. This have been done with the experimental characterization of the cells and the testing of their performance with the design of sensors that can be launched along with the balloon . Additionally, a theoretical approach to the level of insulation required and whether a radiation filter was needed were studied.

It can be determined that the objective related to the **development of a design to measure voltage and current** have been reached with the implementation of the Arduino sensors that measure current and voltage and to store their values whenever it is required. However, all the experiments have been done by feeding the Arduino UNO board with the computer and, because of its excessive weight, carrying a computer inside the box that will be attached to the high altitude balloon is not a good solution. Therefore an external battery will be needed as well as the implementation of a microSD card reader chip along with a microSD card.

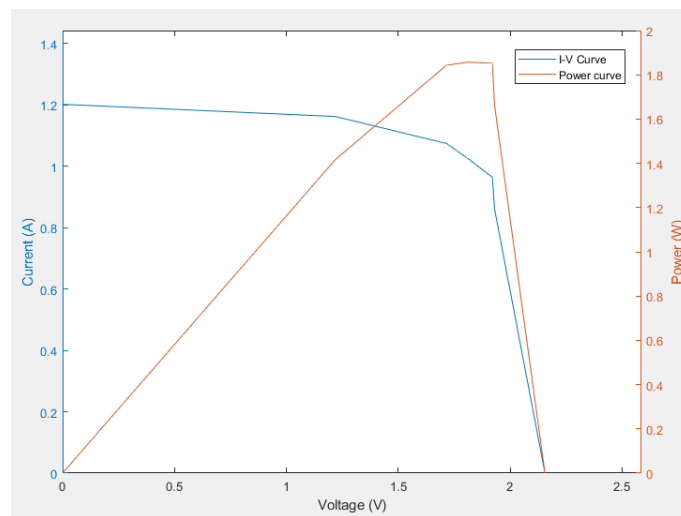


Fig. 12.1. Experimental I-V and power curves

Following the implementation of the sensors that will measure current and voltage during the experiment of the balloon, the next objective of the **characterization of the solar cells** that have been bought has also been accomplished, as the curve obtained using the Arduino and Matlab design defines the correlation between the voltage and the current giving good values of voltage, current and power.

However, the error between the ideal curve obtained by using the Matlab software and the experimental curve could be reduced by considering the factors that affect it. Mainly, this

gap affects the efficiency, as the ideal one is around 19% and the experimental efficiency is slightly above 15%. Although the efficiency is still in the range specified by the manufacturer, it could be increased by improving the assembly process of the solar cells, so that the dirtiness level of the cells is as low as possible. Another factor that affected the experimental efficiency was that the tests were performed without the insulation model. If the array of cells would have been isolated and insulated before the experiments, particles such as dust or fingerprints due to the manipulation of the cells would not be on the solar cells.

Furthermore, obtaining the voltage and current variation values with temperature changes have allowed the **study of an insulation model** so that the cells are not going to be damaged when the high altitude balloon elevates and goes through the troposphere and part of the stratosphere. It has been determined that the use of the insulation model of EVA and a Tedlar composite is the best solution as it protects the cells as it has a wider range of temperatures than the gradient the balloon will pass. Also, the implementation of a low iron rolled glass in the front part of the cells supports the objective of insulation as well as it allows the Sun radiation to pass through it and to the cells. The transmittance is very high and the effect of the glass will barely affect the efficiency of the solar cells.

Additionally, it has been decided that a **radiation filter** is not going to be needed as the changes in radiation will not be significantly important because the Ozone layer is located at a higher altitude than the elevation that the balloon is going to reach and therefore, the gas will behave as a natural filter on the excess of UV radiation coming from the Sun.

Finally, it can be concluded that the experimental design developed through the present bachelor thesis satisfies the requirements needed to launch the solar cells on the high altitude balloon and the implementation on the balloon can be done and, consequently, experiments to test the cells at high altitude can be carried out.

13. FUTURE WORKS

After completing the circuit of the experimental design that will be implemented on the high altitude balloon, the disposition of the different elements that are needed to complete the experiments at high altitude have to be determined, as well as the definition of the experiments that are going to be carried out.

The high altitude balloon carries a payload, which is the name of the combination of the box, where the sensors and tools to perform the experiments at high altitude, and the rope that joins together the box with the balloon. The box has the dimensions specified in Figure 13.1. Knowing these measures, the disposition of the cells can be decided. First of all, the angle of the cells with respect to the box has to be determined. As it has been proven during the experiments developed and explained in Chapters 7 and 8, the optimum angle of incidence is 0° . However, this is a difficult task to decide on the balloon project as the box will ascend vertically, and the angle of incidence will change. Additionally, the balloon will take around three hours to complete the whole flight, so the position of the Sun at the time of the launching has to be taken into account.

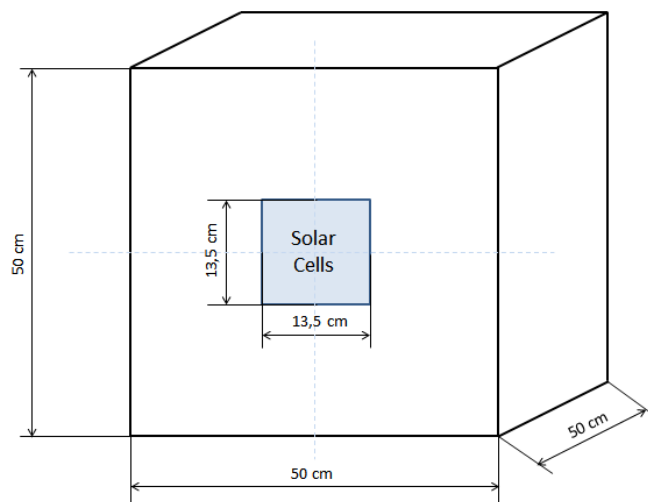


Fig. 13.1. Payload measures

Something else that needs to be considered is the rotation movements of the payload during the flight, not forgetting the addition of a counterweight on the opposite side of the box. Then, in order to pass the wires that connect the solar cells with the Arduino, a small perforation must be done and properly insulated.

Afterwards, the experiments with the high altitude balloon can be carried out. These experiments can obtain data of how monocrystalline solar cells perform when temperature and radiation change with altitude and determine how to improve their performance so

they can be considered a reliable source of energy in works that require a continuous supply of electricity during a long period of time, such as solar cells on mountains or other elevated places, satellites or spaceships.

Currently, there are open investigations on new methods of making the most of solar energy, such as a study on how to put solar cells orbiting around the Earth so they can obtain energy from the Sun and then transmit all that energy to the Earth so it can be used with lasers or microwaves [49]. This way, energy could be sent to any part of the world, even places with limited access or with scarce energy resources. In order to generate a significant amount of electricity out of photovoltaic solar energy, numerous solar panels have to be assembled and therefore a big terrain is occupied. By sending the photovoltaic cells to space and finding a way to use that energy would solve that problem. Besides, the complicated meteorological conditions of the Earth would be avoided, such as the clouds that cover the Sun most of the time during the Winter.

The improvement of the efficiency of photovoltaic cells and will suppose an exponential growth of the photovoltaic energy, making it economically feasible and accessible to the whole population.

BIBLIOGRAPHY

- [1] *Cuántos satélites hay alrededor de la tierra*, 2016. [Online]. Available: <http://www.curiosfera.com/cuantos-satelites-alrededor-la-tierra/>.
- [2] *Sun: Our star*, 2018. [Online]. Available: <https://solarsystem.nasa.gov/solar-system/sun/overview/>.
- [3] W. A. B. John A. Duffie, *Solar engineering of thermal processes*, 4th ed. Wiley, 1991.
- [4] K. Tate, *Proton fusion, the sun's power source, explained (infographic)*, 2014. [Online]. Available: <https://www.space.com/26956-proton-fusion-sun-power-source-infographic.html>.
- [5] *Estructura y composición del sol*. [Online]. Available: <http://www.astromia.com/solar/estrucsol.htm>.
- [6] *Blackbody*, 2016. [Online]. Available: <https://www.britannica.com/science/blackbody>.
- [7] *Electromagnetic spectrum*. [Online]. Available: <https://sites.google.com/site/chempendix/em-spectrum>.
- [8] V. Badescu, *Modeling solar radiation at the earth's surface: Recent advances*, 2008.
- [9] A. T. Mecherikunnel, J. A. Gatlin, and J. C. Richmond, "Data on total and spectral solar irradiance," *Appl. Opt.*, vol. 22, no. 9, pp. 1354–1359, May 1983. doi: 10.1364/AO.22.001354. [Online]. Available: <http://ao.osa.org/abstract.cfm?URI=ao-22-9-1354>.
- [10] M. J. Brian Palmer, *The dept. of solar radiation management*, 2015. [Online]. Available: <https://www.nrdc.org/onearth/dept-solar-radiation-management>.
- [11] *The astronomical pacemaker*. [Online]. Available: <http://www.highstand.org/erohling/DarkMed/ch5.html>.
- [12] A. da Rosa, *Chapter 12 - solar radiation*, Third Edition, A. da Rosa, Ed. Boston: Academic Press, 2013, pp. 485–532. doi: <https://doi.org/10.1016/B978-0-12-397219-4.00012-6>. [Online]. Available: <http://www.sciencedirect.com/science/article/pii/B9780123972194000126>.
- [13] D. R. Myers, Third Edition. New Mexico: CRC Press, 2013.
- [14] D. P. Stern, *Kepler's three laws of planetary motion*. [Online]. Available: <https://www-spf.gsfc.nasa.gov/stargaze/Kep3laws.htm>.
- [15] K. N. Liou, *Chapter 3 - absorption and scattering of solar radiation in the atmosphere*, Second Edition. San Diego, California: Elsevier Science, 2013.

- [16] Á. Méndez, *Composición química de la atmósfera*, 2010. [Online]. Available: <https://quimica.laguia2000.com/quimica-ambiental/composicion-quimica-de-la-atmosfera>.
- [17] *Atmosphere - diagram*. [Online]. Available: <https://www.weatheronline.co.uk/reports/wxfacts/Atmosphere---Diagram.htm>.
- [18] T. E. of Encyclopaedia Britannica, *Photoelectric effect*, 2018. [Online]. Available: <https://www.britannica.com/science/photoelectric-effect>.
- [19] T. Wofford, *Hertz, einstein, and the photoelectric effect*, 2008. [Online]. Available: <https://physicstoday.scitation.org/doi/full/10.1063/1.2930718>.
- [20] *Photoelectric effect equation with problems*, 2016. [Online]. Available: <http://physicsabout.com/photoelectric-effect>.
- [21] “Concerning an heuristic point of view toward the emission and transformation of light,” *Annalen der Physik*, vol. 17, 1905. doi: <http://dx.doi.org/10.1002/andp.19053220607>.
- [22] *Conduction in semiconductors*. [Online]. Available: <https://www.pveducation.org/pvcdrom/conduction-in-semiconductors>.
- [23] N. Mahato, M. O. Ansari, and M. H. Cho, “Production of utilizable energy from renewable resources: Mechanism, machinery and effect on environment,” *Advanced Materials Research*, vol. 1116, pp. 1–32, Aug. 2015. doi: [10.4028/www.scientific.net/AMR.1116.1](https://doi.org/10.4028/www.scientific.net/AMR.1116.1).
- [24] P. Löper *et al.*, “Analysis of the temperature dependence of the open-circuit voltage,” *Energy Procedia*, vol. 27, pp. 135–142, 2012, Proceedings of the 2nd International Conference on Crystalline Silicon Photovoltaics SiliconPV 2012. doi: <https://doi.org/10.1016/j.egypro.2012.07.041>. [Online]. Available: <http://www.sciencedirect.com/science/article/pii/S1876610212012544>.
- [25] E. Cuce, P. M. Cuce, and T. Bali, “An experimental analysis of illumination intensity and temperature dependency of photovoltaic cell parameters,” *Applied Energy*, vol. 111, pp. 374–382, 2013. doi: <https://doi.org/10.1016/j.apenergy.2013.05.025>. [Online]. Available: <http://www.sciencedirect.com/science/article/pii/S0306261913004261>.
- [26] P. Singh and N. Ravindra, “Temperature dependence of solar cell performance—an analysis,” *Solar Energy Materials and Solar Cells*, vol. 101, pp. 36–45, 2012. doi: <https://doi.org/10.1016/j.solmat.2012.02.019>. [Online]. Available: <http://www.sciencedirect.com/science/article/pii/S0927024812000931>.
- [27] *Solar cell i-v characteristic and the solar cell i-v curve*. [Online]. Available: <http://www.alternative-energy-tutorials.com/energy-articles/solar-cell-i-v-characteristic.html>.

- [28] A. Davidson, "Common types of solar cells," *Alternative Energy Solutions*, 2018. [Online]. Available: <http://www.altenergy.org/renewables/solar/common-types-of-solar-cells.html>.
- [29] *Different types of solar panels for home use*. [Online]. Available: <http://www.outdoorliving.online/best-solar-panels/>.
- [30] M. A. Green, "Third generation photovoltaics: Solar cells for 2020 and beyond," *Physica E: Low-dimensional Systems and Nanostructures*, vol. 14, no. 1, pp. 65–70, 2002. doi: [https://doi.org/10.1016/S1386-9477\(02\)00361-2](https://doi.org/10.1016/S1386-9477(02)00361-2). [Online]. Available: <http://www.sciencedirect.com/science/article/pii/S1386947702003612>.
- [31] D. König *et al.*, "Hot carrier solar cells: Principles, materials and design," *Physica E: Low-dimensional Systems and Nanostructures*, vol. 42, no. 10, pp. 2862–2866, 2010, 14th International Conference on Modulated Semiconductor Structures. doi: <https://doi.org/10.1016/j.physe.2009.12.032>. [Online]. Available: <http://www.sciencedirect.com/science/article/pii/S138694770900650X>.
- [32] *Clima madrid: Temperatura, climograma y tabla climática para madrid*, 2018. [Online]. Available: <https://es.climate-data.org/location/92/>.
- [33] *Mr watt shop*, 2018. [Online]. Available: <https://www.mrwatt.eu/en/shop/>.
- [34] G. Campa, "Legacy matlab and simulink support for arduino - file exchange - matlab central," 2018. [Online]. Available: <https://es.mathworks.com/matlabcentral/fileexchange/32374-legacy-matlab-and-simulink-support-for-arduino?focused=6202592&tab=function>.
- [35] L. Llamas, *Opciones para alimentar arduino con baterías*, 2016. [Online]. Available: <https://www.luisllamas.es/alimentar-arduino-baterias/>.
- [36] —, *Leer o escribir en una tarjeta sd o microsd con arduino*, 2016. [Online]. Available: <https://www.luisllamas.es/tarjeta-micro-sd-arduino/>.
- [37] R. Roth, M. Hofmann, and C. Wode, "Geostrophic wind, gradient wind, thermal wind and the vertical wind profile – a sample analysis within a planetary boundary layer over arctic sea-ice," *Boundary-Layer Meteorology*, vol. 92, no. 2, 1999. doi: [10.1023/A:1001850123085](https://doi.org/10.1023/A:1001850123085). [Online]. Available: <https://doi.org/10.1023/A:1001850123085>.
- [38] *Weather forecast maps: Ventusky*. [Online]. Available: <https://www.ventusky.com/?p=40.45;-3.60;8&l=clouds-low&t=20180530/18>.
- [39] M. Panjwani and D. Ghous Bakhsh Narejo, "Effect of altitude on the efficiency of solar panel," vol. 2, 2014.
- [40] "Propiedades termicas de etilenvinilacetato (eva) comparado con poliestireno (ps) y polipropileno (pp)," *Universidad Nacional de Colombia*, [Online]. Available: <https://es.scribd.com/document/332566215/Propiedades-Eva#>.

- [41] *Tpt - tedlar polyester tedlar*. [Online]. Available: <http://sinovoltatics.com/learning-center/materials/tpt-tedlar-polyester-tedlar-what-is-it/>.
- [42] “Materiales transparentes aislantes (tim),” *Revolución silenciosa*, [Online]. Available: <http://cyberevolution-j1972.blogspot.com/2011/10/materiales-transparentes-aislantes-tim.html>.
- [43] K. Cafe, *Electronic warfare and radar systems engineering handbook*. [Online]. Available: <http://www.rfcafe.com/references/electrical/ew-radar-handbook/electro-optics.htm>.
- [44] W. Knaupp and E. Mundschauf, “Solar electric energy supply at high altitude,” *Aerospace Science and Technology*, vol. 8, no. 3, pp. 245–254, 2004. DOI: <https://doi.org/10.1016/j.ast.2003.12.001>. [Online]. Available: <http://www.sciencedirect.com/science/article/pii/S127096380300138X>.
- [45] H. A. Kazem and M. Chaichan, “The impact of using solar colored filters to cover the pv panel in its outcomes,” vol. 2, pp. 464–469, Aug. 2016.
- [46] N. Jain, S. Bagga, and K. Sudhakar, “Effect of color filter on the performance of solar photovoltaic module,” *Proceedings of 2013 International Conference on Power, Energy and Control, ICPEC 2013*, Feb. 2013.
- [47] “What light wave do solar panels use?,” [Online]. Available: <http://www.solarpoweristhefuture.com/what-light-wave-do-solar-panels-use.shtml>.
- [48] O. V. Semenova *et al.*, “Antireflection and protective films for silicon solar cells,” *IOP Conference Series: Materials Science and Engineering*, vol. 66, no. 1, p. 012 049, 2014. [Online]. Available: <http://stacks.iop.org/1757-899X/66/i=1/a=012049>.
- [49] “Un futuro brillante para la energía solar desde el espacio,” *Mundo Solar*, 2012. [Online]. Available: <http://www.dforcesolar.com/energia-solar/un-futuro-brillante-para-la-energia-solar-desde-el-espacio/>.

A. ANNEX I

```
1 clc; clear all;clear workspace;
2
3 %% Assumptions
4 Voc = 0.65; % Volts
5 Ac=3.8e-03;% cell area in m2
6 Isc = 1.55; % Amperes
7
8 Tnoct = 50+273; % Kelvin nominal operation cell temperature
9 Tamb = 25+273;% ambient temperture converted to Kelvin
10
11 G = 1000;% global radiation
12 q = 1.602e-19;% electron charge
13 k = 1.381e-23;% Boltzmann constant
14
15 %% Correlations
16
17 Tc = Tamb + (Tnoct - 20)*G/800;
18 Io = Isc / (exp(q*Voc/(k*Tc))-1);%assumption: the dark sat current of
    the diode depends on Voc and Isc
19
20
21 V = linspace(0,Voc,100); %in order to plot I we need to give values to
    V; we know the min and max values
22 I = Isc -Io*(exp(q*V/(k*Tc))-1);%to obtain the current
23
24 P=V.*I; %to obtain the power values from current and voltage
25 Pmax = max(P);
26 maxEff= Pmax/(Ac*G)*100; %in percentage
27
28 %% I-V and Power curves
29
30 yyaxis left
31 plot(V,I)%I-V curve
32
33 axis([0 Voc+0.2*Voc 0 Isc+0.2*Isc])
34 xlabel('Voltage (V)')
35 ylabel('Current (I)')
36 title('I-V Curve','FontSize',12)
37
38 yyaxis right
39 plot(V,P)%Power curve
40 ylim([0 1.5])
41 ylabel('Power (W)')
```